frontiers | Frontiers in Plant Science

TYPE Original Research
PUBLISHED 06 August 2025
DOI 10.3389/fpls.2025.1639169

OPEN ACCESS

EDITED BY
Claudio Bonghi,
University of Padua, Italy

REVIEWED BY
Irene Romero,
Spanish National Research Council (CSIC), Spain
Jorge Queiroz,
University of Porto, Portugal

*CORRESPONDENCE
Lia-Tânia Dinis
liatdinis@utad.pt
Sandra Pereira
sirp@utad.pt

RECEIVED 01 June 2025
ACCEPTED 03 July 2025
PUBLISHED 06 August 2025

CITATION
Pereira S, Monteiro A, Baltazar M, Maia C, Pereira S, Oliveira MJ, Pádua L, Gonçalves I, Soares B, Branco Z, Moura R, Balfagón D, Moutinho-Pereira J and Dinis L-T (2025) Modulating grapevine performance and hormonal dynamics under summer stress by the synergistic effects of kaolin and silicon. *Front. Plant Sci.* 16:1639169. doi: 10.3389/fpls.2025.1639169

Modulating grapevine performance and hormonal dynamics under summer stress by the synergistic effects of kaolin and silicon

Sandra Pereira[1,2]*, Ana Monteiro[1,2], Miguel Baltazar[1,2], Carolina Maia[1], Sara Pereira[1], Manuel João Oliveira[3], Luís Pádua[1,2], Igor Gonçalves[3], Bruno Soares[3], Zélia Branco[1], Renata Moura[1], Damián Balfagón[4], José Moutinho-Pereira[1,2] and Lia-Tânia Dinis[1,2]*

[1]Centre for the Research and Technology of Agro-Environmental and Biological Sciences (CITAB), University of Trás-os-Montes e Alto Douro (UTAD), Vila Real, Portugal, [2]Inov4Agro - Institute for Innovation, Capacity Building and Sustainability of Agri-Food Production, University of Trás-os-Montes e Alto Douro (UTAD), Vila Real, Portugal, [3]ADVID- Associação para o Desenvolvimento da Viticultura Duriense | CoLAB Vines & Wines, Parque de Ciência e Tecnologia de Vila Real – Régia Douro Park, Vila Real, Portugal, [4]Departmento de Biología, Bioquímica y Ciencias Naturales, Universitat Jaume I, Castellón de la Plana, Spain

Introduction: Climate change is intensifying heat and drought stress in viticulture, negatively impacting yield and grape quality. High temperatures accelerate sugar accumulation and reduce organic acids, disrupting wine balance. Drought also lowers grapevine resilience by reducing stomatal conductance and photosynthetic efficiency, highlighting the need for sustainable strategies. This study evaluated the effects of foliar applications of kaolin (Kl) and silicon (Si) mixtures on grapevine physiology and fruit quality under summer stress.

Methods: The experiment was conducted over two seasons (2023–2024) in a commercial vineyard (Quinta de Ventozelo, Douro Region) using the Touriga Franca variety. Treatments included a control and four formulations (MiKS 1 to 4), all with 2% Kl and Si ranging from 2% to 8%. Physiological measurements included gas exchange, chlorophyll a fluorescence, and leaf water potential. Biochemical analyses assessed pigments, sugars, proteins, phenols, flavonoids, *ortho*-diphenols, and leaf anatomy. Hormonal profiling (abscisic acid (ABA), indole-3-acetic acid (IAA), jasmonic acid (JA), and salicylic acid (SA)) was also performed.

Results: Si and Kl treatments, particularly MiKS 3 and MiKS 4, significantly enhanced gas exchange parameters, water potential, and chlorophyll fluorescence under high-stress conditions. These treatments also increased chlorophyll, carotenoids, cuticular waxes, and cuticle thickness, contributing to improved plant vitality and stress resilience. Secondary metabolites such as *ortho*-diphenols were also enhanced. Hormonal profiling showed increased

ABA and JA and decreased IAA and SA, suggesting strengthened stress signalling and defence responses.

Discussion: Overall, Si and Kl mixtures effectively mitigated summer stress, improving grapevine physiological, biochemical, and anatomical responses under challenging climate conditions.

KEYWORDS

foliar application, grapevine resilience, heat and drought stress, kaolin, photosynthetic efficiency, secondary metabolites, silicon

Highlights

- Si and Kl foliar sprays improved vine resilience to summer stress.
- Higher Si doses enhanced photosynthesis and gas exchange at midday.
- Treatments increased flavonoids, phenols, and ortho-diphenols in leaves.
- Si and Kl improved water potential and leaf anatomical traits.
- Hormonal shifts supported improved stress response and growth balance.

1 Introduction

Global climate change has leading to rising temperatures and decreasing water availability, which pose significant challenges to producing high-quality wine grapes, especially in regions that are already warm and dry. When daily maximum temperatures exceed 35°C, commonly known as "hot days", grapevines decline in essential physiological functions (Keller, 2020). This heat exposure compromises grape quality by reducing the main organic compounds, such as organic acids and anthocyanins, while increased sugar concentrations, increasing the alcohol content in wine. These imbalances are undesirable for winemakers who aim to produce balanced wine flavours (Gutiérrez-Gamboa et al., 2021; Suter et al., 2021). Water availability complicates this scenario, as the majority of vineyards remain unirrigated, exposing grapevines to the natural drought cycles. While moderate water stress can improve grape quality by promoting the synthesis of metabolites like anthocyanins and phenolics (Ju et al., 2019; Yang et al., 2020), severe and prolonged heat and drought events negatively impact grapevine growth, yield, and fruit metabolism, thus threatening both local production and the global distribution of viable winegrowing regions (Keller et al., 2016; Galat et al., 2019; Venios et al., 2020).

Research has extensively investigated grapevine responses to water stress (Flexas et al., 2002; Medrano et al., 2003; Dayer et al., 2013, 2016; Keller et al., 2016). However, relatively less attention has been on heat stress alone (Sadras and Soar, 2009; Soar et al., 2009; Carvalho et al., 2015) and even less studies examine the combined effects of heat and water stress on grapevines (Edwards et al., 2011; Sadras et al., 2012; Rocheta et al., 2014). Among the few studies examining this combined effect, findings have shown that grapevines experiencing water deficit are more susceptible to heat stress, exhibiting more severe declines in physiological responses such as stomatal conductance, pre-dawn leaf water potential, and net photosynthesis. These stresses can lead to significant leaf area loss, further impairing the grapevine's capacity to tolerate long high temperature periods (Edwards et al., 2011). According to Sadras et al. (2012), water and heat stress together have a consistent effect on the plasticity of stomatal conductance. Water deficit reduces stomatal conductance under all environmental conditions, whereas elevated temperatures enhance both conductance and photosynthesis when conditions support a high rate of gas exchange.

These studies underscore the importance of management strategies that can mitigate the combined effects of drought and heat. Foliar applications of kaolin (Kl) and silicon (Si) have emerged as promising approaches to enhance grapevine resilience, reducing losses in quality and yield in the context of increasing climate variability. Indeed, these treatments work by reducing leaf temperature, minimizing water loss, and strengthening the plant's natural defences, thereby decreasing the need for chemical treatments as well as supporting sustainable viticulture.

Kaolin ($Al_2Si_2O_5(OH)_4$), a white, non-toxic aluminosilicate clay, forms a reflective film when applied to leaves, deflecting harmful ultraviolet and infrared radiation while protecting photosystem II from excessive solar exposure (Shellie and King, 2012; Sharma et al., 2015). In grapevines, kaolin reduces leaf temperature and can improve grape quality by stimulating anthocyanin and flavonoid synthesis through activation of the phenylpropanoid and flavonoid pathways, while total soluble solids have shown a variation according to grape variety and time of application, with some studies reporting enhanced soluble solids following early applications, while others note greater effects with later treatments (Conde et al., 2016; Dinis et al., 2016; Dinis et al., 2018a; Kok and Bal, 2018; Luzio et al., 2021; Bernardo et al., 2022).

Silicon, one of Earth's most abundant elements, is not essential for plant survival (Epstein, 1994) but it is widely recognized for enhancing plant resilience/adaptation to both biotic and abiotic stresses (Schabl et al., 2020). When applied through Si-based fertilizers, silicon improves grapevine tolerance by regulating pH, optimizing nutrient uptake, and inducing beneficial biochemical, physiological, and genetic adaptations that enhance stress resistance (Etesami and Jeong, 2018; Jain et al., 2017; Oliva et al., 2020; Rastogi et al., 2021; Pereira et al., 2024).

The combined application of kaolin and silicon in vineyard management provides a promising, low-impact approach to mitigating the effects of climate change on grapevine health and grape quality. The present study evaluates the effects of combining 2% kaolin mixed with various Si concentrations, ranging from 2 to 8%, on grapevine physiology, biochemistry, and grape quality. During the veraison and maturation periods in 2023 and 2024, an experimental study was conducted analysing predawn leaf water potential, gas exchange parameters (stomatal conductance, transpiration rate, net CO_2 assimilation rate, intrinsic water use efficiency, and the Ci/Ca ratio), and chlorophyll a fluorescence (ϕPSII, qP, F_v/F_m, and NPQ). Leaves from different treatments during veraison and maturation were subjected to laboratory analyses, namely biochemical parameters (pigments, phenols, flavonoids, ortho-diphenols, sugars, and protein content) and histological parameters (total leaf thickness, upper and lower cuticle, upper and lower epidermis, palisade and spongy mesophyll cells, and mesophyll thickness).

By investigating these treatments, we aim to advance resilient viticultural practices that improve grapevine tolerance to climate variability, thereby contributing to the sustainability of wine production in climate-sensitive regions as the Douro Region.

2 Materials and methods

2.1 Climate conditions

The experiment was conducted in a commercial vineyard "Quinta de Ventozelo" (41° 18.954′ N 8° 38.940′ W), located in Ervedosa do Douro, in the Cima Corgo sub-region, which has a moderate Mediterranean climate, with hot, dry summers and mild, wet winters, making it ideal for producing high-quality Port and Douro wines. Meteorological conditions (precipitation, and minimum, average and maximum temperatures) prevailing during the experimental period are presented in Figure 1. These data were collected by a weather station located within the vineyard.

Climate data from 2023 revealed a gradual increase in average temperature, rising from approximately 17°C in April to a maximum of 26°C in August, then decreasing to 8°C in December. Minimum temperatures followed a similar trend, starting at 10°C in April, rising to 18°C in August, and then dropping to 5°C in December. The maximum temperatures also demonstrated the same pattern, reaching a maximum at 35°C in August. The year 2023 was characterised by a below-average precipitation year, with a dry period during summer (Instituto Português do Mar e da Atmosfera (IPMA), 2024). In fact, the highest rainfall was recorded in September and October, though overall levels remained low, with a particularly dry period from July to August where rainfall was absent. This dry period, along with high temperatures, suggests potential water stress for the grapevines, influencing irrigation requirements and physiological responses.

In 2024, the average temperature began at approximately 9°C in January, gradually increased to 26°C in August, and then started to

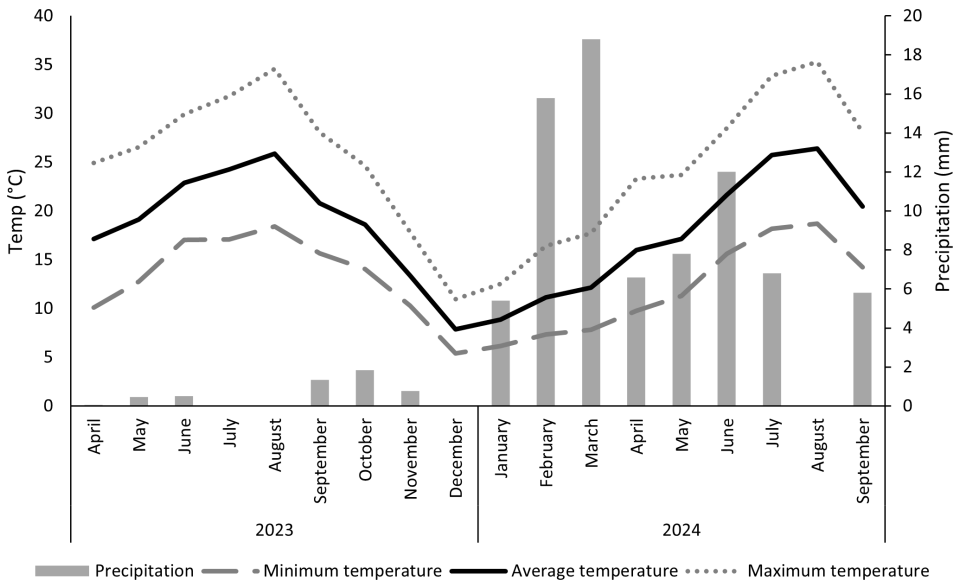

FIGURE 1
Monthly precipitation (mm) and air temperature (minimum, average and maximum) (ºC) from April 2023 to September 2024.

decline, reaching 20°C in September. The minimum temperature followed a similar trend, starting at 6°C in January, to a high 19°C in August, and decreasing to 14°C in September. The maximum temperature was around 13°C in January, 35°C in August, and then dropped to 28°C in September. Regarding precipitation, the highest levels were recorded in March, reaching approximately 19mm, while no rainfall was observed in August. Compared to 2023, the year 2024 was significantly wetter, with much higher precipitation levels.

2.2 Experimental design

The present study was carried out during two growing seasons: 2023 and 2024, in a vineyard planted in 2014 with the Touriga Franca grapevine variety, grafted onto 1103P rootstock. In the first year, four treatments were evaluated: untreated grapevines (control) and grapevines with foliar applications of three different silicon (Si) and kaolin (Kl) formulations. Each formulation contained 2% Kl, with varying Si concentrations ranging from 2% to 6%: MiKS 1- 2% Kl + 2% Si; MiKS 2- 2% Kl + 4% Si; MiKS 3- 2% Kl + 6% Si. The Si concentrations were based on a previous study (Dinis et al., 2024).

The experimental design consisted of three randomized blocks for each treatment, totalling 12 rows. In each row, applications were made to 15 grapevines. In the second year, based on the results obtained in 2023, the treatments were adjusted. Specifically, the MiKS1 treatment was discontinued, and instead, a higher concentration of Si was tested: MiKS 4, containing 2% Kl and 8% Si. The other treatments remained unchanged (Figure 2).

The different formulations were applied twice each year, with a two-week interval between applications, occurring in pre-veraison (mid-June and early July) when the summer stress begun.

2.3 Physiological parameters

2.3.1 Gas exchange measurements

Leaf gas exchange measurements were performed on 3 plants per block, in a total of 9 measurements per treatment by using a portable LCpro + Infrared Gas Analyzer System (IRGA) (ADC BioScientific, Ltd., Hoddesdon, UK), with a 6.25 cm^2 leaf chamber, operating in the open mode, on well-exposed leaves during the morning (09:00–10:30 a.m.) and solar noon (2:00–3:30 p.m.), in veraison (27 July 2023 and 18 July 2024) and maturation stages (24 August 2023 and 29 August 2024).

Net CO_2 assimilation rate (A), stomatal conductance (g_s), and transpiration rate (E) were estimated from gas exchange measurements, using the equations developed by Von Caemmerer and Farquhar (1981). Intrinsic water-use efficiency was calculated as the ratio of A to gs (A/g_s) (Iacono et al., 1998) and the ratio Ci/Ca was also calculated.

FIGURE 2
Experimental design of the field study conducted over two years (2023 and 2024), including the following treatments: untreated grapevines (control) and grapevines receiving foliar applications of four different silicon (Si) and kaolin (Kl) formulations. Each formulation contained 2% kaolin with varying silicon concentrations ranging from 2% to 8%: MiKS 1 – 2% Kl + 2% Si; MiKS 2 – 2% Kl + 4% Si; MiKS 3 – 2% Kl + 6% Si; MiS 4 – 2% Kl + 8% Si.

2.3.2 Chlorophyll a fluorescence measurement

The chlorophyll *a* fluorescence measurement was evaluated on the same leaves and stages used for gas exchange measurements (3 measurements per block, in a total of 9 per treatment). A pulse amplitude modulated fluorimeter was used (Mini-PAM, Photosynthesis Yield Analyzer; Walz, Effeltrich, Germany). The maximum quantum efficiency of photosystem II (*PSII*) was calculated as $F_v/F_m = (F_m–F_0)/F_m$ by measuring the fluorescence signal from a dark-adapted leaf when all reaction centres are open using a low-intensity pulsed measuring light source (F_0) and during a pulse saturating light (0.7 s pulse of 15000 µmol·m^{-2}·s^{-1} of white light) when all reactions centres are closed (F_m). Leaves were dark-adapted for 30 min using dark-adapting leaf-clips for these measurements. Following F_v/F_m estimation, after a 20 s exposure to actinic light (1500 µmol·m^{-2}·s^{-1}), light-adapted steady-state fluorescence yield (F_s) was averaged over 2.5 s, followed by exposure to saturating light (15000 µmol·m^{-2}·s^{-1}) for 0.7 s to establish F_m'. The sample was then shaded for 5s with a far-red light source to determine F_0'. From these measurements, several fluorescence attributes were calculated (Bilger and Schreiber, 1986; Genty et al., 1989): photochemical quenching ($qP=(F_m'–F_s)/(F_m'–F_0')$), non-photochemical quenching ($NPQ = (F_m – F_m')/F_m$) and efficiency of electron transport as a measure of the quantum effective efficiency of *PSII* ($\Phi PSII = \Delta F/F_m' = (F_m' - F_s)/F_m'$). The apparent electron transport rate (Marinari et al., 2007) was estimated as $ETR = (\Delta F/F_m')$ x *PPFD* x 0.5 x 0.84, where PPFD is the photosynthetic photon flux density incident on the leaf, 0.5 is the factor that assumes equal distribution of energy between the two photosystems, and the leaf absorbance used was 0.84 because is the most common value for C3 plants (Bilger and Schreiber, 1986).

2.3.3 Predawn leaf water potential

Predawn leaf water potential (Ψ) was determined with a pressure chamber (model PMS 600, Albany, USA) (Scholander et al., 1965) in veraison and maturation stages. Measurements were performed on nine fully expanded leaves per treatment at predawn (3 measurements per block, in a total of 9 leaves per treatment).

Aerial surveys were conducted only in 2024 to assess canopy reflectance and temperature during veraison. Two unmanned aerial vehicles (UAVs) were used: the Mavic 3T (DJI, Shenzhen, China) and the P4 Multispectral (DJI, Shenzhen, China). The Mavic 3T was used to acquire high-resolution RGB (12 MP) and thermal infrared (TIR) imagery using an uncooled VOx microbolometer with a pixel pitch of 12 µm. UAV flights were performed on 18 July (veraison stage) at three time points (09:30, 11:55, and 13:30 local time) corresponding to early morning, mid-morning and solar noon, following the same flight plan: 40 m height above the ground level, 90% imagery longitudinal overlap, and 80% imagery lateral overlap.

The P4 Multispectral UAV acquires data across five spectral bands using monochrome sensors for blue (450 ± 16 nm), green (560 ± 16 nm), red (650 ± 16 nm), red edge (730 ± 16 nm), and near-infrared (NIR, 840 ± 26 nm). An integrated spectral sunlight sensor recorded incoming irradiance to enable radiometric correction. A single flight survey was conducted at 12:30 at 50 m height form the take-off point with 80% longitudinal and 70% lateral imagery overlap. Prior to the flight, images of a reflectance target were captured to enable radiometric calibration of the multispectral data.

During the TIR flights, dry and wet reference temperatures were collected using a handheld infrared thermometer on sun-exposed leaves. For the dry reference, petroleum jelly was applied to the abaxial leaf surface to occlude stomata, to minimize transpiration and increasing leaf surface temperature. The wet reference was obtained by applying water to similar leaf surfaces, with temperature measured immediately to capture the evaporative cooling effect.

UAV imagery was processed in Pix4Dmapper (Pix4D SA, Lausanne, Switzerland). Separate projects were created for each flight, with the spatial alignment across datasets being ensured. The outputs included RGB orthophoto mosaics, a digital surface model (DSM), a digital terrain model (DTM), land surface temperature (LST) rasters from TIR imagery, and radiometrically calibrated reflectance rasters for each multispectral band.

The RGB data had a spatial resolution of 0.009 m, TIR data 0.0365 m, and multispectral data 0.0278 m.

Subsequently, the computed raster products were imported into QGIS for further analysis. For each treatment and replicate, a 10-m section of vineyard row was selected. From the central part of each row, a central line was estimated and buffered into a 0.2 m wide polygon, then segmented into 20 sub-polygons (0.5 m × 0.2 m). These were used to extract canopy temperature data. The median temperature of each polygon was calculated to reduce the influence of outliers, such as soil pixels or shaded areas. Polygons with missing plants or low vegetative vigour were excluded.

The empirical crop water stress index (CWSI) (Idso et al., 1981) was calculated using the extracted temperature data and temperature dry and wet references. Mean CWSI values, computed from the polygon medians within each replicate, were used for statistical analysis as well as the median temperature in each performed flight.

For spectral reflectance analysis, a canopy surface model (CSM) was calculated from the subtraction of the DTM altitude values to the DSM. Pixels with a CSM height above 0.8 m were considered canopy, and their mean reflectance values across each of the five spectral bands were extracted.

2.4 Leaf biochemistry

Each year, at both the veraison and maturation stages, three leaves per block (totalling nine leaves per treatment) were randomly collected and immediately preserved in liquid nitrogen. In the laboratory, the leaves were ground using liquid nitrogen and then stored at -80°C until analysis. All leaf analyses are expressed on a fresh weight basis.

2.4.1 Photosynthetic pigments

To quantify the photosynthetic pigments, 10 mg of fresh leaf tissue (FW) was combined with 4 ml of 80% acetone. The mixture was then centrifuged at 1,753 x *g* for 10 minutes at 4°C. Post-

centrifugation, absorbance readings were taken at 663 nm, 645 nm, and 470 nm using a SPECTRUM star Nano spectrophotometer (BMG Labtech GmbH, Germany). Given the light and temperature sensitivity of these pigments, all extraction and quantification steps were performed on ice and shielded from light. Pigment concentrations were calculated according to Arnon (1949) and Lichtenthaler (1987), with results expressed in mg g^{-1} FW.

2.4.2 Soluble sugars

To quantify soluble sugars, 10 mg of each sample was extracted in 5 ml of 80% ethanol. The extracts were homogenized and heated at 80°C in a water bath for 60 minutes, then centrifuged at 15,777 *g* to collect the supernatant. Next, 250 µL of each sample was mixed with 750 µL of anthrone reagent. The mixture was chilled at 4°C for 10 minutes, followed by incubation at 100°C for 20 minutes. Absorbance was measured at 625 nm (Leyva et al., 2008). A glucose standard curve was used for quantification, and results were expressed as mg g^{-1} FW.

2.4.3 Soluble proteins

Soluble proteins were extracted using a phosphate-based extraction buffer (pH 7.5; Fisher Scientific, Loughborough, UK) supplemented with EDTA (ethylenediaminetetraacetic acid; Panreac, Barcelona, Spain). The working solution contained this extraction buffer along with PMSF (phenylmethanesulfonyl fluoride; Panreac, Barcelona, Spain) and PVP (polyvinylpyrrolidone; Sigma, St. Louis, MO, USA). Protein quantification followed the Bradford method (Bradford, 1976), with absorbance measured at 595 nm. Soluble protein content was expressed as milligrams of bovine serum albumin equivalents per gram of fresh weight (mg BSAE g^{-1} FW).

2.4.4 Secondary metabolites

To determine the secondary metabolites in the leaves, a methanolic extract at a concentration of 4 mg ml^{-1} was prepared and used for the following quantifications.

Total phenols were quantified using the Folin–Ciocalteu method, with absorbance measured at 725 nm (Rodrigues et al., 2015). Results were expressed in milligrams of gallic acid equivalents per gram of fresh weight (mg GAE g^{-1} FW).

Total flavonoid content in the extracts was quantified using the aluminium chloride ($AlCl_3$) complex method, with absorbance measured at 510 nm, as described by Rodrigues et al. (2015). Results were expressed as milligrams of catechin equivalents per gram of fresh weight (mg CAE g^{-1} FW).

Ortho-diphenols were measured by reading the absorbance at 370 nm, following the method described by Granato et al. (2015). A gallic acid standard curve was used for calibration, and results were expressed as milligrams per gram of fresh weight (mg g^{-1} FW).

2.5 Phytohormones

The contents of abscisic acid (ABA), indole-3-acetic acid (IAA), jasmonic acid (JA), and salicylic acid (SA) were determined using high-performance liquid chromatography coupled with a triple quadrupole mass spectrometer (Micromass®, Manchester, UK) via an orthogonal Z-spray electrospray ion source (Durgbanshi et al., 2005). Lyophilized samples (20 mg) of leaves were extracted in 2.0 mL of distilled water using a mill ball apparatus (MillMix20, Domel, Železniki, Slovenia). [$^2H_6$]-ABA, [$^2H_5$]-IAA, dihydrojasmonic acid (DHJA) and [$^{13}C_6$]-SA (Sigma-Aldrich, USA) were used as internal standards.

After centrifugation at 10,000 × g, the supernatants were collected, and the pH was adjusted to 2.8–3.2 with 30% acetic acid. Extracts were partitioned twice with diethyl ether, and the resulting supernatants were evaporated under vacuum using a centrifuge concentrator (Speed Vac, Jouan, Saint Herblain Cedex, France) at room temperature. The dry residue was resuspended in 500 µL of a 9:1 water:methanol solution, filtered through 0.22 µm PTFE filters, and directly injected into an ultra-performance liquid chromatography system (Waters™ Acquity SDS, Waters Corporation, Milford, MA, USA) interfaced with a TQD triple quadrupole mass spectrometer (Micromass® Ltd., Manchester, UK).

Chromatographic separation was performed on a reversed-phase C18 column (Gravity, 50 × 2.1 mm, 1.8 µm particle size; Macherey-Nagel GmbH, Germany) using a methanol:water gradient supplemented with 0.1% acetic acid at a flow rate of 300 µL min^{-1}. The aqueous phase was maintained at 90% for the first 2 minutes, decreased to 10% over 6 minutes, then increased back to 90% by 7 minutes, and held constant until the end of the 8-minute run.

Mass spectrometry was conducted in multiple reaction monitoring mode using nitrogen as the drying and nebulizer gas (cone gas flow: 250 L h^{-1}; desolvation flow: 1200 L h^{-1}) and argon as the collision gas. Cone voltage and collision energies were set according to Durgbanshi et al. (2005), with minor modifications. Data processing was carried out using MassLynx™ v4.1 software, and phytohormone concentrations (ng g^{-1} DW) were determined by interpolating the response ratios of the phytohormones to their internal standards against a calibration curve prepared with commercial ABA, IAA, JA, and SA standards.

2.6 Histological parameters

Anatomical tissue measurements were conducted on nine mature leaves per treatment, with three leaves collected from each of the three blocks. Leaf samples were collected from the central region to minimize variability in thickness. After fixation in formalin aceto-alcohol for 24 hours, the samples underwent dehydration, clearing, and paraffin embedding. Transverse sections (4 µm thick) were then prepared using a rotary microtome (Leica RM 2135, Germany). These sections were mounted on slides and stained with 0.1% toluidine blue. Tissue thickness was measured using an inverted optical microscope (Olympus IX51, Olympus Corporation, Tokyo, Japan) and analysed with Digimizer image analysis software (MedCalc Software, Ostend, Belgium).

2.7 Statistical analyses

Data analysis was performed using the SPSS 20.0 software (SPSS Software, Chicago, IL, USA). After testing for analysis of variance (ANOVA) assumptions, statistical differences among treatments within each developmental stage and year were evaluated by one-way factorial ANOVA, followed by the *post hoc* Tukey test. Different letters represent significant differences ($P< 0.05$) among the applied formulations.

3 Results

The results of this study highlight the significant impact of combining Kl and Si on grapevine physiology, biochemical composition, and anatomical adaptations under heat and drought stress conditions. The differential effects observed across treatments indicate that Si and Kl formulations play a critical role in enhancing plant resilience by modulating physiological responses, optimizing water use, improving photosynthetic efficiency, and strengthening biochemical defences.

3.1 Kaolin – silicon mixtures boost physiological responses in grapevines under summer stress

The gas exchange and chlorophyll *a* fluorescence parameters of treated plants with various mixtures of Kl and Si foliar applications were analysed during the morning and solar noon periods at the veraison and maturation phenological stages in both 2023 and 2024. The results are presented in Tables 1, 2, respectively.

Additionally, the predawn water potential was assessed at both the veraison and maturation stages in 2023 and 2024, as shown in Figure 3.

In the veraison of 2023, during the morning measurements, significant differences were observed only in *gs* (Table 1), where MiKS 2-treated plants had significantly higher *gs* than those treated with MiKS 3, with an increase of 43.8%. For the solar noon period, MiKS 1-treated plants showed the lowest values for *gs*, *E*, and *A*. Compared to MiKS 1, untreated plants exhibited significantly higher *E* and *gs*, with increases of 81.0% and 84.4%, respectively. MiKS 2-treated plants displayed significantly higher *gs* and *A* values than both MiKS 1 (98.7% and 90.2% increases, respectively) and MiKS 3 (54.7% and 51.7% increases, respectively). Additionally, MiKS 2-treated plants showed significantly higher *A* values compared to the control, with an increase of 35.0%. Regarding chlorophyll *a* fluorescence, during the same period, *NPQ* showed the only significant difference, presented MiKS 2-treated plants 69.9%, 67.3% and 69.1% lower values compared to control, MiKS 1 and MiKS 3 plants.

In maturation stage of 2023, during the morning measurements, control plants exhibited significantly higher *E* and *gs* values than MiKS 1-treated plants (252.4% and 112.4% increases, respectively) and MiKS 3-treated plants (310.7% and 253.1% increases, respectively). MiKS 2-treated plants also exhibited significantly higher *gs* and *E* compared to both MiKS 1 and MiKS 3, with increases of 108.3% and 246.2% for *gs*, and 113.5% and 148.7% for *E*, respectively. Similar results were observed for *A*, with MiKS 2-treated plants having significantly higher values than MiKS 1 and MiKS 3-treated plants, with increases of 112.3% and 172.7%, respectively. During the solar noon period, MiKS 2-treated plants exhibited the highest values for *gs*, *E*, and *A*, with increases of 305.0% (*gs*), 398.3% (*E*), and 205.5% (*A*) compared to MiKS 3-treated plants, which recorded the lowest values. The highest *Ci/Ca* ratio was observed in MiKS 1-treated plants, with a 129.0% increase over the control and a 77.5% increase compared to MiKS 3-treated plants. Regarding chlorophyll *a* fluorescence, on the solar noon period in the maturation of 2023, control plants had the lowest *NPQ* values, with reductions of 33.8% and 36.4% compared to MiKS 1- and MiKS 3-treated plants, respectively.

Regarding predawn leaf water potential, no significant differences were observed in 2023 in either veraison or maturation (Figure 3).

Regarding 2024, during veraison in the morning, plants treated with the mixtures generally showed significantly higher *gs*, *E*, and *A* values. MiKS 3-treated plants had the highest *Ci/Ca* ratio, which was 17.9% higher than MiKS 2 and 15.3% higher than MiKS 4. In the solar noon period, MiKS 4-treated plants had the highest values of *gs*, *E*, *A*, and *A/gs*, while control plants recorded the lowest values. In fact, in comparison to the control, MiKS 4-treated plants increased 322.7% in *gs*, 194.0% in *E*, 272.7% in *A*, and 109.8% in *A/gs*. However, overall, all formulations resulted in increased values of *E*, *gs*, *A*, and *A/gs* during this phenological stage.

Regarding chlorophyll *a* fluorescence during veraison in 2024, significant differences were observed at solar noon. MiKS 3-treated plants had *ΦPSII* values that were 48.9% higher than untreated plants. In terms of F_v/F_m, MiKS 2- and MiKS 3-treated plants displayed significantly higher values compared to control and MiKS 4, with increases ranging from 5.0% to 6.0%. The *NPQ* was significantly higher in treated plants with the higher doses of Si (MiKS 3 and MiKS 4) compared to both control and MiKS 2-treated plants, with increases ranging from 22.7% to 40.4%.

During maturation in 2024, in the morning period, MiKS 3 and MiKS 4-treated plants exhibited significantly higher *gs* values compared to MiKS 2, with increases of 41.8% and 17.9%, respectively. Additionally, MiKS 3-treated plants also had higher *E* (118.1%) and *A* (100.2%) values than control ones. In the solar noon period, all formulations induced an *E* increase compared to control, with increases ranging from 33.0% to 34.0%. However, only MiKS 3 and MiKS 4 (which had the highest Si concentration) showed higher *A/gs* values, with increases of 102.2% and 31.1%, respectively, when compared to untreated plants.

For chlorophyll *a* fluorescence during the morning period in the maturation of 2024, MiKS 3 and MiKS 4-treated plants showed significantly higher *ΦPSII* values than untreated plants, with increases of 39.8% and 41.7%, respectively. On the other hand, *NPQ* values were significantly higher in MiKS 2-treated plants compared to control (26.0%) and MiKS 3 (27.2%).

Finally, significant differences were observed in water potential during 2024. During veraison, plants treated with all Si and Kl

TABLE 1 Gas exchange parameters (mean±SD), namely transpiration rate (*E*, mmol m^{-2} s^{-1}), stomatal conductance (*gs*, mmol m^{-2} s^{-1}), intercellular carbon (*Ci*, µmol mol^{-1}), net CO_2 assimilation rate (*A*, µmol m^{-2} s^{-1}), intrinsic water use efficiency (*A/gs*, µmol mol^{-1}) and intercellular/atmospheric CO_2 concentration ratio (*Ci/Ca*), in veraison and maturation of 2023 and 2024 (morning and solar noon) in Touriga Franca leaves subjected to combined application of KI (2%) and Si (2 to 8%).

Year	Phenological stages	Time	Treatment	*E* (mmol.m^{-2}.s^{-1})	*gs* (mmol.m^{-2}.s^{-1})	*A* (µmol.m^{-2}.s^{-1})	*A/gs* (µmol.mol^{-1})	*Ci/Ca*
2023	Veraison	Morning	**Control**	2.72 ± 0.30	133.7 ± 10.4 ab	11.2 ± 1.2	81.4 ± 2.9	0.655 ± 0.059
			Miks 1 (KI_2% + Si_2%)	2.46 ± 0.31	126.2 ± 18.7 ab	10.2 ± 1.6	84.5 ± 7.2	0.599 ± 0.039
			Miks 2 (KI_2% + Si_4%)	2.65 ± 0.67	158.2 ± 20.4 b	12.5 ± 1.2	79.1 ± 3.4	0.624 ± 0.059
			Miks 3 (KI_2% + Si_6%)	2.14 ± 0.33	110.0 ± 11.5 a	10.9 ± 2.1	85.2 ± 2.6	0.652 ± 0.036
			***P* value**	0.236	0.008	0.229	0.287	0.199
		Solar noon	**Control**	2.95 ± 0.62 b	123.2 ± 22.6 b	8.4 ± 2.0 a	79.2 ± 8.3	0.641 ± 0.047
			Miks 1 (KI_2% + Si_2%)	1.63 ± 0.24 a	66.8 ± 12.3 a	6.0 ± 1.0 a	89.0 ± 6.9	0.618 ± 0.030
			Miks 2 (KI_2% + Si_4%)	2.46 ± 0.78 ab	132.7 ± 13.9 b	11.3 ± 1.3 b	88.3 ± 13.4	0.603 ± 0.019
			Miks 3 (KI_2% + Si_6%)	2.34 ± 0.72 ab	85.8 ± 17.9 a	7.5 ± 1.6 a	86.7 ± 4.9	0.627 ± 0.053
			***P* value**	0.034	<0.001	<0.001	0.452	0.395
	Maturation	Morning	**Control**	2.46 ± 0.63 c	51.2 ± 6.4 b	3.6 ± 1.4 ab	90.9 ± 6.0	0.626 ± 0.083
			Miks 1 (KI_2% + Si_2%)	0.70 ± 0.27 a	24.1 ± 6.2 a	2.4 ± 0.5 a	80.7 ± 6.6	0.625 ± 0.046
			Miks 2 (KI_2% + Si_4%)	1.49 ± 0.27 b	50.2 ± 6.3 b	5.0 ± 1.0 b	90.4 ± 5.7	0.591 ± 0.029
			Miks 3 (KI_2% + Si_6%)	0.60 ± 0.14 a	14.5 ± 3.2 a	1.8 ± 0.7 a	87.6 ± 6.6	0.619 ± 0.021
			***P* value**	<0.001	<0.001	0.003	0.128	0.639
		Solar noon	**Control**	0.47 ± 0.14 a	9.2 ± 2.8 ab	2.3 ± 0.9 a	155.3 ± 32.7	0.283 ± 0.054 a
			Miks 1 (KI_2% + Si_2%)	1.01 ± 0.36 ab	21.2 ± 8.1 ab	1.3 ± 0.2 a	101.7 ± 47.3	0.648 ± 0.036 b
			Miks 2 (KI_2% + Si_4%)	1.50 ± 0.47 b	24.1 ± 9.8 b	3.9 ± 0.8 b	138.6 ± 40.7	0.527 ± 0.153 ab
			Miks 3 (KI_2% + Si_6%)	0.30 ± 0.14 a	6.0 ± 2.7 a	1.3 ± 0.2 a	151.3 ± 21.7	0.365 ± 0.053 a
			***P* value**	0.002	0.012	<0.001	0.264	0.007
2024	Veraison	Morning	**Control**	2.59 ± 0.85 a	73.0 ± 10.9 a	6.6 ± 1.2 a	90.2 ± 12.6	0.583 ± 0.047 ab
			Miks 2 (KI_2% + Si_4%)	4.28 ± 0.46 b	74.2 ± 10.9 a	11.4 ± 1.4 c	114.1 ± 27.0	0.530 ± 0.048 a
			Miks 3 (KI_2% + Si_6%)	4.05 ± 0.42 b	129.7 ± 26.4 b	9.3 ± 1.0 b	113.2 ± 22.1	0.625 ± 0.085 b
			Miks 4 (KI_2% + Si_8%)	4.87 ± 0.96 b	120.5 ± 16.6 b	11.7 ± 1.4 c	102.4 ± 6.0	0.542 ± 0.045 a
			***P* value**	<0.001	<0.001	<0.001	0.322	0.009

(Continued)

10.3389/fpls.2025.1639169

TABLE 1 Continued

Year	Phenological stages	Time	Treatment	*E* (mmol.m^{-2}.s^{-1})	*gs* (mmol.m^{-2}.s^{-1})	*A* (µmol.m^{-2}.s^{-1})	*A/gs* (µmol.mol^{-1})	*Ci/Ca*
		Solar noon	**Control**	0.81 ± 0.35 a	15.0 ± 5.3 a	2.5 ± 0.9 a	103.4 ± 16.2 a	0.504 ± 0.121
			Miks 2 (Kl_2% + Si_4%)	2.08 ± 0.46 b	50.0 ± 9.7 b	5.7 ± 1.4 b	125.5 ± 13.5 ab	0.510 ± 0.073
			Miks 3 (Kl_2% + Si_6%)	2.08 ± 0.55 b	48.6 ± 11.1 b	5.4 ± 0.9 b	161.4 ± 38.7 b	0.525 ± 0.094
			Miks 4 (Kl_2% + Si_8%)	2.39 ± 0.88 b	63.4 ± 18.8 b	9.3 ± 2.8 c	216.9 ± 44.9 c	0.440 ± 0.125
			***P* value**	<0.001	<0.001	<0.001	<0.001	0.484
	Maturation	Morning	**Control**	1.16 ± 0.33 a	94.1 ± 14.1 ab	5.0 ± 1.2 a	83.7 ± 9.8	0.618 ± 0.098
			Miks 2 (Kl_2% + Si_4%)	2.00 ± 0.44 b	86.1 ± 14.3 a	8.1 ± 0.8 b	85.9 ± 5.0	0.626 ± 0.052
			Miks 3 (Kl_2% + Si_6%)	2.53 ± 0.41 c	122.1 ± 11.9 b	9.9 ± 1.2 c	87.9 ± 6.2	0.599 ± 0.034
			Miks 4 (Kl_2% + Si_8%)	2.30 ± 0.20 bc	101.5 ± 34.8 b	9.1 ± 1.2 bc	86.8 ± 12.6	0.615 ± 0.040
			***P* value**	<0.001	0.007	<0.001	0.233	0.776
		Solar noon	**Control**	1.03 ± 0.35 a	25.6 ± 4.8	1.3 ± 0.4	59.2 ± 7.4 a	0.677 ± 0.105
			Miks 2 (Kl_2% + Si_4%)	1.38 ± 0.27 b	27.8 ± 2.3	1.8 ± 0.5	78.9 ± 16.2 ab	0.707 ± 0.095
			Miks 3 (Kl_2% + Si_6%)	1.37 ± 0.34 b	27.2 ± 3.3	2.1 ± 0.7	119.7 ± 29.3 bc	0.585 ± 0.085
			Miks 4 (Kl_2% + Si_8%)	1.38 ± 0.40 b	24.4 ± 3.6	2.1 ± 0.7	136.8 ± 32.1 c	0.597 ± 0.077
			***P* value**	0.025	0.519	0.909	<0.001	0.071

Different letters represent significant differences between the treatments at the same time of day and within the same phenological stage. The absence of letters indicates that there are no significant differences between treatments. n = 9.

10.3389/fpls.2025.1639169

10.3389/fpls.2025.1639169

TABLE 2 Chlorophyll *a* fluorescence parameters (mean ± SD): effective efficiency of PSII (*ΦPSII*), photochemical (*qP*), maximum quantum efficiency of photosystem II (*Fv/Fm*), and non-photochemical (*NPQ*) quenching, in veraison and maturation of 2023 and 2024 (morning and solar noon) in Touriga Franca leaves subjected to combined application of Kl (2%) and Si (2 to 8%).

Year	Phenological stages	Time	Treatment	*ΦPSII*	*Qp*	*Fv/Fm*	*NPQ*
2023	Veraison	Morning	**Control**	0.204 ± 0.083	0.581 ± 0.084	0.800 ± 0.039	8.26 ± 0.55 b
			Miks 1 (Kl_2% + Si_2%)	0.150 ± 0.041	0.571 ± 0.084	0.841 ± 0.041	7.61 ± 2.26 b
			Miks 2 (Kl_2% + Si_4%)	0.205 ± 0.048	0.639 ± 0.080	0.812 ± 0.075	2.49 ± 0.34 a
			Miks 3 (Kl_2% + Si_6%)	0.207 ± 0.037	0.593 ± 0.082	0.839 ± 0.052	8.06 ± 0.88 b
			***P* value**	0.243	0.522	0.487	<0.001
		Solar noon	**Control**	0.159 ± 0.033	0.613 ± 0.094	0.800 ± 0.046	3.27 ± 0.36
			Miks 1 (Kl_2% + Si_2%)	0.127 ± 0.036	0.588 ± 0.025	0.828 ± 0.025	2.94 ± 0.51
			Miks 2 (Kl_2% + Si_4%)	0.117 ± 0.035	0.650 ± 0.079	0.802 ± 0.041	2.98 ± 0.55
			Miks 3 (Kl_2% + Si_6%)	0.138 ± 0.036	0.648 ± 0.086	0.831 ± 0.042	3.58 ± 0.58
			***P* value**	0.307	0.502	0.393	0.170
	Maturation	Morning	**Control**	0.100 ± 0.018	0.634 ± 0.039	0.737 ± 0.028	4.17 ± 0.43
			Miks 1 (Kl_2% + Si_2%)	0.108 ± 0.029	0.560 ± 0.095	0.723 ± 0.065	3.85 ± 0.94
			Miks 2 (Kl_2% + Si_4%)	0.106 ± 0.035	0.634 ± 0.063	0.744 ± 0.053	4.21 ± 0.66
			Miks 3 (Kl_2% + Si_6%)	0.145 ± 0.034	0.618 ± 0.070	0.738 ± 0.073	3.73 ± 0.74
			***P* value**	0.142	0.261	0.934	0.684
		Solar noon	**Control**	0.064 ± 0.033	0.475 ± 0.071	0.736 ± 0.099	3.06 ± 0.79 a
			Miks 1 (Kl_2% + Si_2%)	0.068 ± 0.022	0.576 ± 0.120	0.639 ± 0.097	4.62 ± 1.20 b
			Miks 2 (Kl_2% + Si_4%)	0.063 ± 0.021	0.612 ± 0.126	0.777 ± 0.074	4.17 ± 0.43 ab
			Miks 3 (Kl_2% + Si_6%)	0.087 ± 0.028	0.537 ± 0.082	0.772 ± 0.106	4.81 ± 0.47 b
			***P* value**	0.445	0.280	0.102	0.010
2024	Veraison	Morning	**Control**	0.071 ± 0.048	0.337 ± 0.082	0.866 ± 0.066	5.42 ± 1.17
			Miks 2 (Kl_2% + Si_4%)	0.130 ± 0.046	0.443 ± 0.066	0.890 ± 0.053	6.30 ± 0.71
			Miks 3 (Kl_2% + Si_6%)	0.090 ± 0.051	0.381 ± 0.079	0.861 ± 0.100	6.52 ± 1.01
			Miks 4 (Kl_2% + Si_8%)	0.108 ± 0.045	0.398 ± 0.038	0.908 ± 0.049	6.53 ± 1.33
			***P* value**	0.071	0.182	0.307	0.087
		Solar noon	**Control**	0.088 ± 0.023 a	0.357 ± 0.064	0.875 ± 0.053 a	6.35 ± 1.03 a
			Miks 2 (Kl_2% + Si_4%)	0.116 ± 0.030 ab	0.376 ± 0.068	0.928 ± 0.030 b	6.09 ± 0.81 a
			Miks 3 (Kl_2% + Si_6%)	0.131 ± 0.024 b	0.439 ± 0.110	0.924 ± 0.048 b	7.79 ± 1.05 b
			Miks 4 (Kl_2% + Si_8%)	0.107 ± 0.029 ab	0.408 ± 0.066	0.880 ± 0.057 a	8.55 ± 0.92 b
			***P* value**	0.049	0.229	0.031	<0.001
	Maturation	Morning	**Control**	0.103 ± 0.013 a	0.360 ± 0.046	0.818 ± 0.053	4.31 ± 0.92 a
			Miks 2 (Kl_2% + Si_4%)	0.126 ± 0.033 ab	0.423 ± 0.044	0.795 ± 0.052	5.43 ± 0.62 b
			Miks 3 (Kl_2% + Si_6%)	0.144 ± 0.031 b	0.371 ± 0.059	0.811 ± 0.027	4.27 ± 0.68 a
			Miks 4 (Kl_2% + Si_8%)	0.146 ± 0.026 b	0.378 ± 0.074	0.790 ± 0.042	4.54 ± 0.74 ab
			***P* value**	0.007	0.174	0.507	0.040
		Solar noon	**Control**	0.083 ± 0.014	0.330 ± 0.051	0.784 ± 0.042	6.08 ± 1.15
			Miks 2 (Kl_2% + Si_4%)	0.096 ± 0.026	0.329 ± 0.071	0.771 ± 0.046	6.88 ± 1.20

(Continued)

TABLE 2 Continued

Year	Phenological stages	Time	Treatment	*ΦPSII*	*Qp*	*Fv/Fm*	*NPQ*
			Miks 3 (Kl_2% + Si_6%)	0.102 ± 0.043	0.330 ± 0.050	0.730 ± 0.058	6.22 ± 1.08
			Miks 4 (Kl_2% + Si_8%)	0.101 ± 0.035	0.331 ± 0.052	0.713 ± 0.089	5.57 ± 0.84
			***P* value**	0.647	1.000	0.710	0.158

Different letters represent significant differences between the treatments at the same time of day and within the same phenological stage. The absence of letters indicates that there are no significant differences between treatments. n = 9.

formulations exhibited significantly higher water potential than control plants, with increases of 24.2% for MiKS 2, 42.1% for MiKS 3, and 40.1% for MiKS 4. In the maturation stage, only MiKS 3-treated plants showed a significant increase in water potential compared to untreated plants, with an increase of 17.6%.

The UAV-based TIR imagery acquired at three time points (morning, mid-morning, and solar noon, presented in Figure 4A) during veraison in 2024 showed a variation in grapevine canopy temperature and CWSI among treatments (Table 3). Across all flight periods, control plants presented the highest mean canopy temperatures (30.6°C in early morning, 41.0°C in mid-morning, and 44.4°C at solar noon). However, statistical analysis (P-values: 0.82, 0.75, and 0.77, respectively) revealed no significant differences among treatments. In contrast, MiKS-treated plants showed lower temperatures, with MiKS 2 and MiKS 4 recording the lowest early morning values (29.6 °C and 29.7 °C, respectively).

In the earlier flight, all MiKS treatments showed lower canopy temperatures compared to the control (30.6°C), as presented in the example in Figure 4B. MiKS 2 and MiKS 4 showed the greatest reductions, with a surface temperature decrease of 1.01°C and 0.93°C, respectively. MiKS 3 had a smaller reduction of 0.27°C. At middle-morning flight, the control showed a temperature of 41°C, when comparing to MiKS treatments, MiKS 2 presented the largest decrease (−1.20°C), followed by MiKS 4 (−0.62°C) and MiKS 3 (−0.47°C). At solar noon, all treatments showed lower temperatures than the control (44.4°C), although the differences were generally smaller. MiKS 2 had a 1.16°C reduction, MiKS 3 a 0.47°C reduction, and MiKS 4 a 0.37°C reduction. CWSI values followed a similar trend. The control showed the highest CWSI across all periods, reaching 0.78 at solar noon. MiKS 2 showed the lowest CWSI at all three times (0.40, 0.65, and 0.66), corresponding to reductions of 0.11, 0.10, and 0.12 compared to the control. MiKS 4 also showed CWSI reductions (−0.10 to −0.04), while MiKS 3 values were close to control CWSI values.

The UAV multispectral data (Figure 4C) shows that control plants presented a lower reflectance in the visible bands when compared to all MiKS-treated plants. In the blue band, reflectance was 0.02 in the control, while in all MiKS treatments it was 0.05. Similarly, for the green band, the control treatment presented a mean value of 0.07 compared to 0.09–0.10 in the treated groups, and for the red band, the control (0.04) is lower than the 0.06–0.07 observed in the MiKS treatments. In the red edge band, differences were smaller across treatments, with the control at 0.22 and MiKS treatments at around 0.23. NIR reflectance values were also similar with 0.35 for both the control and MiKS 2, 0.36 for MiKS 3, and 0.34 for MiKS 4.

3.2 Modulation of leaf anatomy and biochemical defence induced by kaolin–silicon mixtures application

The photosynthetic pigments in leaves treated with different Si + Kl formulations during the veraison and maturation stages of 2023 and 2024 are presented in Table 4.

Additionally, Table 5 displays the results for soluble sugars, soluble proteins, and secondary metabolites (total phenols, total flavonoids, and *ortho*-diphenols) analysed in the same leaves and timepoints. Meanwhile, histological parameters of the leaves were also analysed, and the results are presented in Table 6. Regarding the hormonal profile, this was analysed only during the veraison and maturation stages of 2024, and the results are shown in Figure 5.

During the veraison stage in 2023, significant differences were observed across several physiological and biochemical parameters in grapevine leaves. For photosynthetic pigments (Table 4), untreated plants showed the highest levels of chlorophyll *a*, chlorophyll *b*, total chlorophyll, and carotenoids, while MiKS 1-treated plants exhibited the lowest. MiKS 2 and MiKS 3 treatments resulted in intermediate values, being significantly lower than the control but higher than MiKS 1. Regarding sugar content, untreated, MiKS 2-, and MiKS 3-treated plants had significantly higher levels than MiKS 1-treated plants, with increases of 27.7%, 37.3%, and 35.3%, respectively. MiKS 2-treated plants also showed a significant increase in both total phenol content (14.5%) and flavonoid levels (41.4%) in comparison to the control. All treatments significantly enhanced *ortho*-diphenol content compared to control plants, with increases of 13.3% (MiKS 1), 37.1% (MiKS 2), and 36.7% (MiKS 3).

At maturation in 2023, several parameters continued to show significant variation among treatments. Photosynthetic pigment levels remained the lowest in MiKS 1-treated plants. The control plants maintained the highest levels of all pigments except for carotenoids. MiKS 2 and MiKS 3 treatments increased chlorophyll *a* and total chlorophyll levels, with MiKS 2 also leading to a higher carotenoid content. Sugar content (Table 5) followed the same pattern observed in veraison: MiKS 1-treated plants showed the lowest values, while control, MiKS 2, and MiKS 3 treatments resulted in increases of 23.1%, 13.6%, and 22.8%, respectively. MiKS 3-treated plants displayed the highest levels of total phenols, flavonoids, and *ortho*-diphenols. For this treatment, total phenol content increased by 23.2% and 17.8% when compared to MiKS 2 and control, respectively. Flavonoid content also rose by

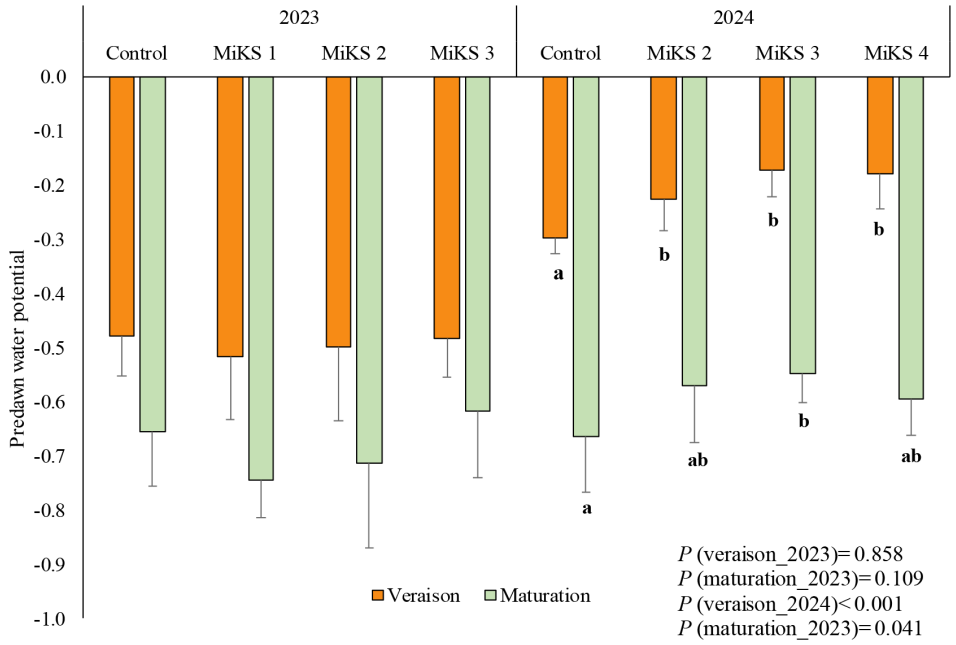

FIGURE 3
Predawn leaf water potential (mean ± SD), in veraison and maturation of 2023 and 2024, in Touriga Franca leaves subjected to combined application of KI (2%) and Si (2 to 8%). Different letters represent significant differences between the treatments within the same phenological stage. The absence of letters indicates that there are no significant differences between treatments. n = 9.

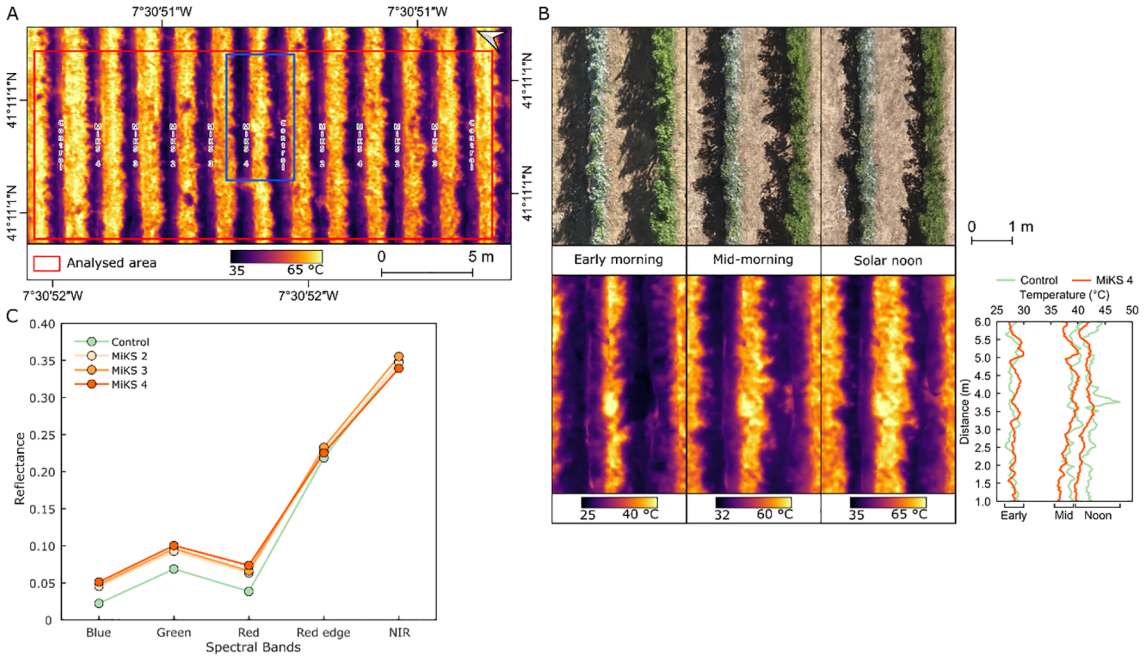

FIGURE 4
Overview of land surface temperature at solar noon **(A)** during veraison in 2024, in Touriga Franca grapevines subjected to combined application of KI (2%) and Si (4 to 8%). Detail of two vineyard rows treated with MiKS 4 and control, corresponding to the blue rectangle in A, shown for all three flights, along with the temperature of profile across six-meter transect within the rows **(B)**. Spectral reflectance in the five multispectral bands acquired by the unmanned aerial vehicle **(C)**, n = 56 for control; n = 58 for MiKS 2; n = 59 for MiKS 3; and n = 50 for MiKS 4 (differences in n due to the exclusion of row sections with missing grapevines).

TABLE 3 Grapevine temperature and crop water stress index (CWSI) values (mean ± SD) from thermal infrared data acquired by unmanned aerial vehicle at three different flight periods in veraison and maturation of 2024, in Touriga Franca leaves subjected to combined application of Kl (2%) and Si (4 to 8%).

Treatment	*Temperature (°C)*			*CWSI*		
	Early morning	*Mid-morning*	*Solar noon*	*Early morning*	*Mid-morning*	*Solar noon*
Control	30.6 ± 0.9	41.0 ± 1.3	44.4 ± 1.2	0.515 ± 0.084	0.753 ± 0.115	0.777 ± 0.128
MiKS 2 (Kl_2% + Si_4%)	29.6 ± 0.9	39.8 ± 1.5	43.2 ± 1.5	0.403 ± 0.111	0.652 ± 0.123	0.655 ± 0.133
MiKS 3 (Kl_2% + Si_6%)	30.4 ± 0.9	40.6 ± 1.1	43.9 ± 1.1	0.485 ± 0.083	0.713 ± 0.125	0.728 ± 0.147
MiKS 4 (Kl_2% + Si_8%)	29.7 ± 0.9	40.4 ± 1.2	44.0 ± 1.1	0.411 ± 0.100	0.701 ± 0.138	0.738 ± 0.143
***P* value**	0.818	0.750	0.769	0.841	0.749	0.771

n = 56 for control; n = 58 for MiKS 2; n = 59 for MiKS 3; and n = 50 for MiKS 4 (differences in n due to the exclusion of row sections with missing grapevines).

36.0%, 17.2%, and 31.1% relative to the control, MiKS 1, and MiKS 2, respectively. Additionally, *ortho*-diphenol levels in MiKS 3-treated plants increased by 29.1%, 10.6%, and 13.0% compared to MiKS 2, MiKS 1, and control, respectively. In the same year, for the histological parameters, significant differences were observed in the upper cuticle and lower cuticle at both phenological stages, with MiKS 2- and MiKS 3-treated plants showing the highest values.

During the veraison stage of 2024, significant differences were found in sugar, protein, flavonoids, *ortho*-diphenols, and phytohormones. Sugar content was significantly higher in all treated plants compared to the control, with increases of 30.8% (MiKS 2), 33.8% (MiKS 3), and 16.5% (MiKS 4). Protein levels were significantly higher in MiKS 2-treated plants than in MiKS 3, with a 20.0% increase. Flavonoid content was highest in MiKS 3-treated plants, exhibiting a 16.9% increase when compared to the control. These plants also showed the highest *ortho*-diphenol content, with a 9.26% increase relative to MiKS 4-treated plants. Phytohormone analysis (Figure 5) revealed that, at veraison, MiKS 2-treated plants had the highest ABA content, showing a 57.4% increase compared to MiKS 4. Furthermore, MiKS 4-treated plants also had the lowest IAA levels, 69.4% lower than the control. JA content was markedly increased in MiKS 3 and MiKS 4 (463.7% and 904.0% increases, respectively, over the control). For SA, MiKS 2 and MiKS 4 treatments showed increases of 65.0% and 30.2%, respectively, compared to MiKS 3, with MiKS 2 also surpassing the control by 37.5%. In this phenological stage, both the upper and lower cuticles exhibited the same pattern as in 2023, with all treated plants showing a significant increase in these parameters compared to the untreated ones (Table 6). Furthermore, MiKS 2-treated plants demonstrated significantly higher palisade mesophyll cell density, total leaf thickness, and mesophyll thickness, while MiKS 4-treated plants consistently displayed the lowest values. Notably, control plants had a significantly thicker upper epidermis than MiKS 2-treated plants, with a 27.4% increase.

At the maturation stage in 2024, significant differences were observed in pigment composition, sugar, protein, phenolic compounds, phytohormones, and histological traits. Carotenoid content was significantly higher in MiKS 4-treated plants than in MiKS 3, with a 46.7% increase (Table 4). Sugar levels were highest in control, MiKS 3-, and MiKS 4-treated plants, all significantly surpassing MiKS 2 with increases of 44.7%, 48.8%, and 17.5%, respectively (Table 5). MiKS 4-treated plants exhibited the highest contents of protein, phenols, flavonoids, and *ortho*-diphenols. Protein content was particularly elevated, with increases of 49.4%, 90.6%, and 50.3% compared to the control, MiKS 2, and MiKS 3, respectively. Similarly, total phenol content was highest in MiKS 4-treated plants, surpassing the control, MiKS 2, and MiKS 3 by 52.7%, 58.9%, and 50.2%, respectively. Flavonoid levels followed a similar pattern, with MiKS 4 showing increases of 70.7%, 60.6%, and 41.9% compared to the control, MiKS 2, and MiKS 3. MiKS 3-treated plants also exhibited significantly higher flavonoid content than the control, with a 20.2% increase. Moreover, MiKS 4-treated plants had the highest *ortho*-diphenol content, exceeding the control, MiKS 2, and MiKS 3 by 31.3%, 38.0%, and 19.2%, respectively. MiKS 3 also had higher content of *ortho*-diphenol than the control (10.2%) and MiKS 2 (15.8%). Phytohormonal analysis (Figure 5) revealed that, at maturation, MiKS 2 maintained the highest ABA levels, with increases of 19.98% and 33.58% compared to control and MiKS 4, respectively. MiKS 3 exhibited the highest IAA content, surpassing the control by 78.8%, MiKS 2 by 102.9%, and MiKS 4 by 44.1%. Relative to the control, JA levels were significantly increased in MiKS 2 (124.2%) and MiKS 4 (65.2%), while MiKS 3 showed a 14.8% decrease. SA content was highest in MiKS 2-treated plants, with increases of 82.0%, 129.7%, and 68.5% compared to control, MiKS 3, and MiKS 4, respectively. Similar to the veraison stage, during maturation, both the upper and lower cuticles maintained the same pattern, with all treated plants showing a significant increase in these parameters compared to untreated ones (Table 6). Moreover, MiKS 3-treated plants exhibited significantly higher palisade mesophyll cell density and, as a result, greater mesophyll thickness, particularly when compared to control plants, with increases of 34.0% and 15.4%, respectively. On the other hand, MiKS 3-treated plants simultaneously displayed the thinnest upper epidermis compared to control plants, with a 26.3% reduction.

4 Discussion

The combination of treatments with Si and Kl demonstrated a significant impact on the ecophysiological and biochemical performance of grapevines, particularly under summer stress

10.3389/fpls.2025.1639169

TABLE 4 Photosynthetic pigments (mean±SD): chlorophyll *a*, *b*, *total* and carotenoids, in veraison and maturation of 2023 and 2024, in Touriga Franca leaves subjected to combined application of Kl (2%) and Si (2 to 8%).

Year	Phenological stages	Treatment	Chlorophyll *a* (mg.g^{-1})	Chlorophyll *b* (mg.g^{-1})	Chlorophyll total (mg.g^{-1})	Carotenoids (mg.g^{-1})
2023	Veraison	**Control**	2.04 ± 0.07 c	1.75 ± 0.03 c	3.79 ± 0.10 c	0.648 ± 0.037 c
		Miks 1 (Kl_2% + Si_2%)	1.31 ± 0.06 a	1.37 ± 0.06 a	2.67 ± 0.11 a	0.279 ± 0.017 a
		Miks 2 (Kl_2% + Si_4%)	1.79 ± 0.08 b	1.56 ± 0.04 b	3.34 ± 0.12 b	0.501 ± 0.035 b
		Miks 3 (Kl_2% + Si_6%)	1.81 ± 0.01 b	1.60 ± 0.02 b	3.40 ± 0.03 b	0.465 ± 0.022 b
		***P* value**	<0.001	<0.001	<0.001	<0.001
	Maturation	**Control**	1.59 ± 0.07 b	1.61 ± 0.12 b	3.20 ± 0.19 b	0.387 ± 0.027 bc
		Miks 1 (Kl_2% + Si_2%)	1.20 ± 0.05 a	1.35 ± 0.03 a	2.55 ± 0.08 a	0.298 ± 0.024 a
		Miks 2 (Kl_2% + Si_4%)	1.57 ± 0.04 b	1.50 ± 0.02 ab	3.07 ± 0.07 b	0.426 ± 0.022 c
		Miks 3 (Kl_2% + Si_6%)	1.52 ± 0.01 b	1.52 ± 0.08 ab	3.04 ± 0.08 b	0.343 ± 0.020 ab
		***P* value**	<0.001	0.016	<0.001	<0.001
2024	Veraison	**Control**	1.59 ± 0.11	1.73 ± 0.22	3.32 ± 0.32	0.485 ± 0.036
		Miks 2 (Kl_2% + Si_4%)	1.73 ± 0.07	1.77 ± 0.09	3.50 ± 0.16	0.444 ± 0.022
		Miks 3 (Kl_2% + Si_6%)	1.57 ± 0.27	1.67 ± 0.21	3.24 ± 0.48	0.447 ± 0.056
		Miks 4 (Kl_2% + Si_8%)	1.71 ± 0.53	1.58 ± 0.12	3.29 ± 0.50	0.525 ± 0.167
		***P* value**	0.301	0.547	0.397	0.544
	Maturation	**Control**	1.33 ± 0.18	1.58 ± 0.23	2.91 ± 0.37	0.273 ± 0.110 ab
		Miks 2 (Kl_2% + Si_4%)	1.36 ± 0.07	1.55 ± 0.08	2.91 ± 0.15	0.331 ± 0.032 ab
		Miks 3 (Kl_2% + Si_6%)	1.23 ± 0.15	1.56 ± 0.25	2.78 ± 0.39	0.240 ± 0.026 a
		Miks 4 (Kl_2% + Si_8%)	1.46 ± 0.13	1.62 ± 0.22	3.08 ± 0.35	0.352 ± 0.038 b
		***P* value**	0.067	0.928	0.499	0.018

Different letters represent significant differences between the treatments at the same time of day and within the same phenological stage. The absence of letters indicates that there are no significant differences between treatments. n = 9.

conditions. The analysis of these parameters revealed that treatments not only optimized water-use efficiency and photosynthetic performance but also enhanced the plant's biochemical defences, improving overall resilience.

4.1 Physiological performance of grapevines under summer stress pulverized by Kaolin–silicon mixtures

The application of Si and Kl significantly improved gas exchange parameters, particularly under abiotic stress conditions. The contrasting *gs* responses observed between 2023 and 2024 can be largely explained by the markedly different climatic conditions registered during both growing seasons. As shown in Figure 1, 2023 was characterized by extremely low precipitation during the vegetative and ripening phases, coupled with consistently high temperatures, particularly during the summer months. These conditions imposed significant water stress on the vines, strongly limiting stomatal conductance. Under such circumstances, MiKS 2 exhibited the highest *gs* values. This formulation may have permitted a more balanced stomatal behaviour. The moderate antitranspirant effect provided by MiKS 2 possibly reduced excessive water loss while still allowing sufficient stomatal opening for gas exchange under severe drought, thus optimizing physiological performance under high vapor pressure deficit conditions. On the other hand, in 2024, precipitation was more frequent throughout the vegetative cycle, with rainfall episodes occurring between April and July. The increased soil water availability likely alleviated water stress, allowing treatments MiKS 3 and MiKS 4 to exert their beneficial effects by mitigating heat load and photoinhibition through increased leaf reflectance. The increase in stomatal conductance led to a higher *A* due to greater CO_2 uptake, which consequently also resulted in an increased *E* (Table 1). These findings confirm the role of Si in maintaining stomatal functionality during periods of high temperatures, potentially by enhancing water uptake and transport (Laane, 2018), which positively influences photosynthesis (Khan et al., 2017; Tripathi et al., 2017). Additionally, Si role in enhancing the synthesis of aquaporins might also support its role in improving water uptake, which would further enhance gas exchange under heat stress (Wang et al., 2021). Moreover,

10.3389/fpls.2025.1639169

TABLE 5 Primary and secondary metabolites (mean±SD): soluble sugars, soluble protein, total phenols, flavonoids, and *ortho*-diphenols, in veraison and maturation of 2023 and 2024, in Touriga Franca leaves subjected to combined application of Kl (2%) and Si (2 to 8%).

Year	Phenological stages	Treatment	Soluble sugars ($mg.g^{-1}$)	Soluble protein ($mg.g^{-1}$)	Total phenols ($mg.g^{-1}$)	Total flavonoids ($mg.g^{-1}$)	*Ortho*-diphenols ($mg.g^{-1}$)
2023	Veraison	**Control**	31.8 ± 1.0 b	1.47 ± 0.10	17.5 ± 0.5 a	5.53 ± 0.08 a	32.4 ± 0.4 a
		Miks 1 (Kl_2% + Si_2%)	24.9 ± 2.3 a	1.48 ± 0.16	18.9 ± 1.1 ab	6.68 ± 0.29 b	36.7 ± 0.6 b
		Miks 2 (Kl_2% + Si_4%)	34.2 ± 2.2 b	1.52 ± 0.14	20.1 ± 1.1 b	7.82 ± 0.80 c	44.4 ± 1.3 c
		Miks 3 (Kl_2% + Si_6%)	33.7 ± 2.0 b	1.42 ± 0.11	19.4 ± 1.0 ab	6.84 ± 0.09 bc	44.3 ± 0.8 c
		***P* value**	<0.001	0.632	0.048	0.001	<0.001
	Maturation	**Control**	41.5 ± 2.6 c	1.58 ± 0.11	17.5 ± 0.6 ab	5.36 ± 0.09 a	37.0 ± 1.6 b
		Miks 1 (Kl_2% + Si_2%)	33.7 ± 1.7 a	1.60 ± 0.14	18.9 ± 0.8 bc	6.22 ± 0.18 a	37.8 ± 1.3 b
		Miks 2 (Kl_2% + Si_4%)	38.3 ± 1.2 b	1.68 ± 0.10	16.7 ± 0.2 a	5.56 ± 0.01 a	32.4 ± 1.2 a
		Miks 3 (Kl_2% + Si_6%)	41.4 ± 1.9 c	1.72 ± 0.13	20.6 ± 0.9 c	7.29 ± 0.71 b	41.8 ± 0.9 c
		***P* value**	<0.001	0.199	<0.001	<0.001	<0.001
2024	Veraison	**Control**	32.8 ± 1.3 a	1.51 ± 0.10 ab	16.6 ± 1.8	4.43 ± 0.25 a	31.0 ± 1.9 ab
		Miks 2 (Kl_2% + Si_4%)	42.9 ± 1.8 c	1.74 ± 0.14 c	15.9 ± 0.9	4.48 ± 0.17 ab	31.2 ± 1.0 ab
		Miks 3 (Kl_2% + Si_6%)	43.9 ± 1.2 c	1.45 ± 0.08 a	17.6 ± 1.7	5.18 ± 0.18 c	33.1 ± 1.6 b
		Miks 4 (Kl_2% + Si_8%)	38.2 ± 1.4 b	1.63 ± 0.09 bc	18.0 ± 1.9	4.72 ± 0.19 b	30.3 ± 1.1 a
		***P* value**	<0.001	<0.001	0.150	<0.001	0.019
	Maturation	**Control**	35.6 ± 1.2 c	1.62 ± 0.15 a	16.6 ± 1.9 a	3.51 ± 0.42 a	26.5 ± 1.2 a
		Miks 2 (Kl_2% + Si_4%)	24.6 ± 2.1 a	1.27 ± 0.11 a	16.0 ± 1.9 a	3.73 ± 0.25 ab	25.2 ± 1.1 a
		Miks 3 (Kl_2% + Si_6%)	36.6 ± 1.7 c	1.61 ± 0.05 a	16.9 ± 2.1 a	4.22 ± 0.49 b	29.2 ± 1.8 b
		Miks 4 (Kl_2% + Si_8%)	28.9 ± 1.3 b	2.42 ± 0.40 b	25.4 ± 0.8 b	5.99 ± 0.75 c	34.8 ± 1.5 c
		***P* value**	<0.001	<0.001	<0.001	<0.001	<0.001

Different letters represent significant differences between the treatments at the same time of day and within the same phenological stage. The absence of letters indicates that there are no significant differences between treatments. n = 9.

Kl may have contributed to this effect by improving photosynthetic activity under drought and heat stress, as supported by Cataldo et al. (2022). Pilon et al. (2013) reported that an increase in *A* in Si-treated plants was associated with higher *gs* and increased concentrations of chlorophyll *a* and carotenoids. Interestingly, in this study, grapevines treated with the highest Si concentration, particularly MiKS 4, exhibited increased *gs* and higher carotenoid levels during maturation in 2024 (Table 3). Although chlorophyll *a* levels also increased, the differences were not statistically significant. Higher stomatal conductance allows for greater stomatal opening, enhancing CO_2 assimilation and increasing photosynthesis, as CO_2 is essential for glucose production in the Calvin cycle. However, this increase also leads to higher water loss through *E*. While increased *gs* improves CO_2 uptake, plants must regulate water loss to maintain water-use efficiency (Giorgi et al., 2019). Thus, the formulation MiKS 4 played a role in keeping stomatal function active, increasing photosynthesis and transpiration and enabling greater gas exchange. The trade-off between photosynthesis and water loss is a complex adaptive mechanism that may be modulated by the enhanced efficiency of the cuticle, as shown in the histological analysis (Table 6).

Although statistically significant increases in *A/gs* ratio were observed specifically at solar noon during both veraison and maturation in 2024, these results suggest that, under certain phenological stages and peak irradiance periods, combined application with Si and Kl may contribute to a more efficient water use. Indeed, several studies have reported improvements in water use efficiency across a variety of crops following foliar Si application (Ma et al., 2004; Gunes et al., 2008; Ming et al., 2012; Ali et al., 2013; Amin et al., 2014; Ahmed et al., 2014; Kurdali et al., 2013; Dehghanipoodeh et al., 2018). This enhancement is often attributed to increased leaf and epidermal tissue thickness due to the deposition of a silica double layer (Gong et al., 2003). The deposition of Si not only strengthens the cuticular layer but also may contribute to improved water retention in leaf tissues, directly supporting the plants' ability to withstand water stress. Similarly, Kl application has also been reported to improve water use efficiency in vineyards by reducing water loss through the lowering of leaf temperature (Glenn et al., 2010; Jifon and Syvertsen, 2003), although variable responses have been observed in other studies (Segura-Monroy et al., 2015).

TABLE 6 Histological parameters (mean ± SD): total leaf thickness, upper and lower cuticle, upper and lower epidermis, palisade and spongy mesophyll cells, and mesophyll thickness, in veraison and maturation of 2023 and 2024, in Touriga Franca leaves subjected to combined application of Kl (2%) and Si (2 to 8%).

Year	Phenological stages	Treatment	Total leaf thickness (μm)	Upper cuticle (μm)	Lower cuticle (μm)	Upper epidermis (μm)	Lower epidermis (μm)	Palisade mesophyll cells (μm)	Spongy mesophyll cells (μm)	Mesophyll thickness (μm)
2023	Veraison	**Control**	122.0 ± 12.9	2.81 ± 0.39 a	2.40 ± 0.12 a	11.7 ± 2.0	13.3 ± 2.6	43.2 ± 5.4	48.7 ± 9.9	91.9 ± 13.5
		Miks 1 (Kl_2% + Si_2%)	125.4 ± 9.3	3.14 ± 0.29 ab	2.43 ± 0.19 a	12.8 ± 1.6	14.2 ± 4.2	40.1 ± 4.1	52.7 ± 9.7	92.8 ± 9.2
		Miks 2 (Kl_2% + Si_4%)	134.9 ± 16.9	3.32 ± 0.21 b	2.87 ± 0.27 b	12.0 ± 1.7	16.6 ± 4.5	46.7 ± 8.4	53.4 ± 9.1	100.1 ± 16.4
		Miks 3 (Kl_2% + Si_6%)	139.7 ± 15.6	3.38 ± 0.16 b	2.93 ± 0.27 b	12.0 ± 2.9	14.5 ± 3.6	43.9 ± 3.6	63.1 ± 8.4	107.0 ± 11.6
		***P* value**	0.135	0.008	<0.001	0.780	0.482	0.275	0.080	0.183
	Maturation	**Control**	125.5 ± 18.2	2.81 ± 0.23 a	2.40 ± 0.24 a	14.9 ± 3.3	12.7 ± 5.4	40.8 ± 7.1	51.8 ± 11.0	92.6 ± 12.9
		Miks 1 (Kl_2% + Si_2%)	129.0 ± 8.4	3.13 ± 0.18 b	2.75 ± 0.27 ab	13.3 ± 2.6	14.1 ± 2.5	41.8 ± 4.3	54.0 ± 8.5	95.8 ± 7.5
		Miks 2 (Kl_2% + Si_4%)	130.7 ± 15.6	3.59 ± 0.22 c	2.93 ± 0.28 b	14.3 ± 2.2	14.5 ± 3.9	46.2 ± 9.3	49.3 ± 7.0	95.5 ± 12.7
		Miks 3 (Kl_2% + Si_6%)	137.5 ± 20.8	3.72 ± 0.15 c	2.92 ± 0.24 b	14.8 ± 2.5	16.2 ± 2.8	45.4 ± 6.9	54.4 ± 14.9	99.9 ± 21.4
		***P* value**	0.644	<0.001	0.007	0.716	0.487	0.488	0.831	0.854
2024	Veraison	**Control**	173.6 ± 10.9 ab	3.47 ± 0.45 a	3.01 ± 0.46 a	15.8 ± 3.0 b	14.2 ± 3.8	54.7 ± 6.0 a	82.3 ± 11.0	137.0 ± 9.0 a
		Miks 2 (Kl_2% + Si_4%)	188.2 ± 22.5 b	4.25 ± 0.61 b	3.72 ± 0.56 b	12.4 ± 2.6 a	13.4 ± 2.6	66.7 ± 16.4 b	87.8 ± 15.8	154.4 ± 19.7 b
		Miks 3 (Kl_2% + Si_6%)	178.6 ± 15.3 ab	4.59 ± 0.60 b	3.61 ± 0.44 b	12.9 ± 2.8 ab	15.0 ± 3.3	49.4 ± 3.9 a	93.1 ± 14.0	142.5 ± 14.6 ab
		Miks 4 (Kl_2% + Si_8%)	169.1 ± 12.3 a	4.36 ± 0.55 b	3.61 ± 0.67 b	14.9 ± 3.7 ab	13.3 ± 2.3	48.7 ± 6.6 a	84.2 ± 6.6	133.0 ± 11.9 a
		***P* value**	0.033	<0.001	0.010	0.023	0.480	<0.001	0.168	0.004
	Maturation	**Control**	163.4 ± 13.9	2.98 ± 0.33 a	2.49 ± 0.42 a	16.0 ± 3.5 b	14.7 ± 4.4	49.1 ± 5.9 a	78.1 ± 11.7	127.3 ± 13.9 a
		Miks 2 (Kl_2% + Si_4%)	177.9 ± 18.4	4.21 ± 0.59 b	3.48 ± 0.45 b	13.8 ± 2.6 ab	12.2 ± 2.5	55.9 ± 9.0 a	88.3 ± 16.6	144.2 ± 18.9 ab
		Miks 3 (Kl_2% + Si_6%)	181.1 ± 22.3	4.50 ± 0.50 b	3.78 ± 0.63 b	11.8 ± 2.5 a	14.1 ± 3.9	65.8 ± 9.4 b	81.1 ± 15.4	146.9 ± 18.9 b
		Miks 4 (Kl_2% + Si_8%)	177.8 ± 15.3	4.52 ± 0.40 b	3.38 ± 0.38 b	13.1 ± 2.1 ab	13.1 ± 2.2	55.2 ± 9.1 a	88.5 ± 14.6	143.7 ± 14.9 ab
		***P* value**	0.083	<0.001	<0.001	0.005	0.304	<0.001	0.226	0.026

Different letters represent significant differences between the treatments at the same time of day and within the same phenological stage. The absence of letters indicates that there are no significant differences between treatments.
n = 9.

10.3389/fpls.2025.1639169

Predawn leaf water potential is widely recognized as a simple yet reliable physiological indicator for assessing grapevine water status (Levin, 2019; Tuccio et al., 2019). The absence of significant differences in predawn water potential among treatments in 2023, despite the severe drought conditions, suggests that under extreme water deficit, the capacity of the applied treatments to improve vine water status may be limited. In such conditions, soil water availability may be so low that any potential benefit from treatments like Si and Kl is overridden by the prevailing water scarcity. On the other hand, the increases in predawn water potential in 2024 (Figure 3) for treated plants suggest, in agreement with *A/gs*, that these treatments helped the plants maintain a better water status, which is critical for survival during drought periods. In fact, in the present study, the water potential exhibited a similar trend to *gs*, *A*, and *E*, as all these parameters are closely regulated by stomatal behaviour, which is influenced by the plant's water status. When water availability is high, stomata remain open, facilitating gas exchange and optimizing both photosynthesis and transpiration (Zhu et al., 2023). This suggests that the treatments did not only preserve stomatal function but also improved the plant's internal hydraulic conductance, further supporting better water retention and efficiency. An increase in water potential as a result of Si application has been also reported in studies across various crops (Gong and Chen, 2012; Ming et al., 2012; Hattori et al., 2007). According to Rizwan et al. (2015), Si accumulates in the leaf epidermis forming a physical barrier that reduces water loss. Similarly, the improvement in plant water status through Kl application under stress conditions, as reported in several studies (Glenn et al., 2010; Denaxa et al., 2012; Boari et al., 2015; Nanos, 2015; AbdAllah, 2017; Dinis et al., 2018a; Brito et al., 2018, 2019), is mainly attributed to the formation of a reflective particle film on the leaf surface, which lowers leaf temperature and helps maintain higher leaf water potential under stress.

According to Ojeda et al. (2001), the level of water stress experienced by a plant can be assessed based on baseline water potential values. In this study, the grapevines were classified as experiencing moderate water stress at veraison in 2023. By veraison in 2024, water potential values had become less negative across all treatments, with treated plants even reaching a state of hydric comfort (0 to -0.3 MPa). Although similar trends were observed in the control group, the significant increases observed in treated plants suggest an improved capacity for water retention, helping to mitigate the negative effects of water stress and sustain physiological functions during critical phenological stages. However, as the maturation stage progressed, water potential values dropped below -0.6 MPa in both years, indicating that the plants were subjected to moderate water stress at this stage (Ojeda et al., 2001). Nevertheless, the treatments with MiKS 2 and MiKS 3 showed slightly higher values than -0.6 MPa, in maturation 2024. Prichard et al. (2004) have suggested that moderate water stress in red wine grape varieties was beneficial for improving must quality, as it stimulates the synthesis of polyphenols, aromatic compounds and other beneficial compounds, particularly during veraison. This controlled stress encourages the development of complex flavours and the accumulation of compounds that contribute to the wine's colour, tannin structure, and aromatic profile. However, excessive water availability can disrupt this beneficial stress response. By increasing water supply, the mobilization of photoassimilates to the berries is reduced, which may hinder the concentration of key compounds and negatively affect fruit quality, potentially leading to wines with less intensity and complexity (Magalhães, 2015).

In 2023, extreme drought and heat likely triggered a protective downregulation of PSII efficiency in grapevines, masking potential treatment effects. On the contrary, during veraison and maturation in 2024, plants treated with MiKS 3 and MiKS 4 demonstrated higher $\Phi PSII$ values (Table 2), which can be related to the protection of the photosynthetic apparatus (Qin et al., 2016). Indeed, this increase suggests that treatments applied in the current study improved photosynthetic efficiency, allowing the plants to maximize their energy production despite stressful environmental conditions. These treatments showed reduced susceptibility to photoinhibition, likely due to the enhanced efficiency of photosystem II and, in some cases, a greater capacity for efficient photochemical quenching (Dinis et al., 2018a). This improvement is probably linked to increased sucrose concentration in the leaves (as observed in the present study), enhanced sucrose transport, and greater phloem loading ability (Conde et al., 2016, 2018). Furthermore, this enhanced photochemical efficiency could also be partly attributed to the hormonal shifts induced by the treatments, particularly the reduction in ABA and the increase in IAA, which together support a more resilient photosynthetic system under stress (Li et al., 2019; Muller et al., 2021). Recent studies conducted on table grapes and wheat in dry and arid climates have confirmed the beneficial effects on fluorescence parameters after the application of Si (Maghsoudi et al., 2015; Nascimento et al., 2022). Indeed, both studies revealed that the plants suffered less damage to the photosynthetic apparatus, improving their performance when subjected to water and heat stress conditions. Similarly, Kl application can positively influence *PSII* functionality by acting as a reflective barrier, reducing excess light absorption and lowering leaf temperature (Azuara et al., 2023). Kl helps prevent the overexcitation of chlorophyll molecules by reflecting a portion of the incoming solar radiation, thus reducing the risk of photoinhibition and oxidative stress in the photosynthetic machinery (Rosati et al., 2006). The general increase in *NPQ* observed in plants treated with Si + Kl, especially during veraison in 2024, suggests an improved capacity to dissipate the excess of light energy as heat through non-photochemical quenching mechanisms. This process is crucial under stress conditions, as it allows plants to safely release the surplus energy that cannot be used for photochemistry, thereby preventing the overexcitation of chlorophyll molecules and the generation of reactive oxygen species (ROS) (Murakami et al., 2024).

UAV-based TIR data (Table 3) demonstrated that foliar application of Kl and Si, contributed to reduced canopy temperature and showed lower CWSI values during veraison in 2024, particularly in MiKS 2-treated plants. Although the differences were not statistically significant, the reduction in canopy temperature and CWSI values across treated grapevines

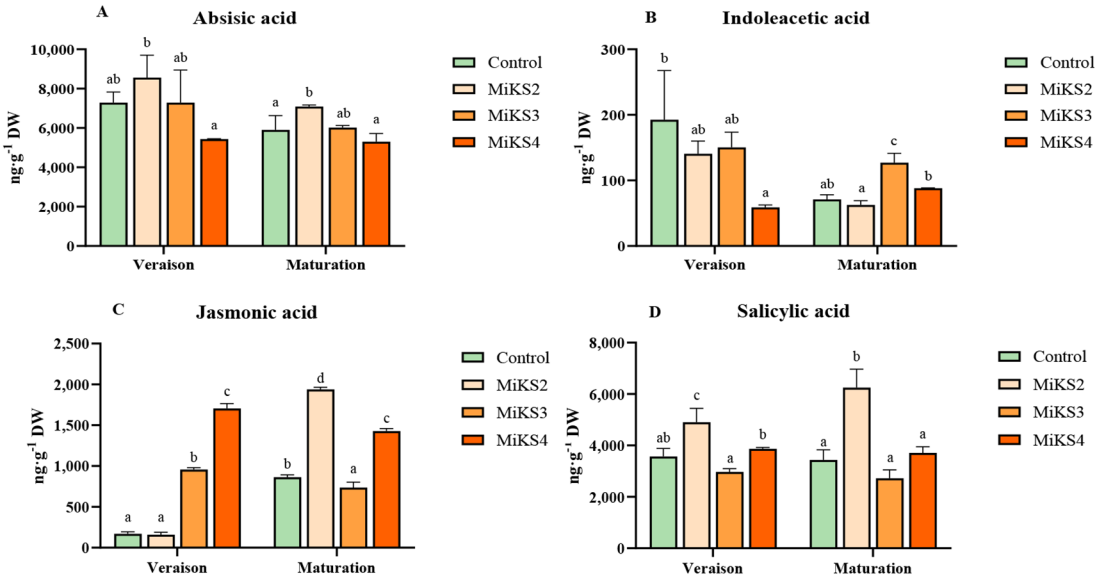

FIGURE 5
Hormonal profile (mean ± SD): **(A)** abscisic acid, **(B)** indoleacetic acid, **(C)** jasmonic acid, and **(D)** salicylic acid, in veraison and maturation of 2023 and 2024, in Touriga Franca leaves subjected to combined application of Kl (2%) and Si (2 to 8%). Different letters represent significant differences between the treatments within the same phenological stage. The absence of letters indicates that there are no significant differences between treatments. n = 9.

suggests an improved capacity to buffer physiological stress under high thermal load. In the early morning, MiKS 2 and MiKS 4 showed the greatest temperature reductions compared to the control, indicating an improved canopy cooling at the start of the day. Mid-morning measurements revealed that foliar treatments continued to moderate canopy warming as solar radiation increased. At solar noon (Figure 4A), despite peak thermal stress, all treatments maintained slightly lower values than the control, with MiKS 2-treated plants showing the greatest difference and the most consistent effects across temperature and CWSI, demonstrating suitability to improve grapevine resilience under climate-related stress conditions. These observations point to a cumulative mitigation effect, whereby foliar applications reduced the impact of thermal stress during the critical periods (Rodrigues et al., 2025). Multispectral reflectance data (Figure 4C) further support the influence of Kl and Si treatments on canopy physiology and structure (Okhrimenko et al., 2019). Treated grapevines showed higher reflectance in the visible bands (blue, green, and red) compared to the control, which may be indicative of changes in pigment concentration or leaf surface characteristics, as observed in this work (Tables 4, 6) (Cabello-Pasini and Macías-Carranza, 2011; Albetis et al., 2018). Among the treatments, MiKS 2-treated plants presented slightly lower green and red reflectance compared to MiKS 3 and MiKS 4, which may reflect a dose-dependent effect of Si on pigment-related traits. In the red edge and NIR bands, all treatments showed similar reflectance values. Overall, the integration of UAV-based TIR and multispectral data demonstrated that Kl and Si foliar applications modulate both canopy temperature dynamics and optical properties, serving as a complementary approach to conventional measurements (Pádua et al., 2022). These remotely sensed indicators align with higher *gs*, *A*, and predawn water potential observed in the treated grapevines (Table 1, Figure 3). UAV-based data thus provide a scalable, non-destructive means to assess vine physiological status and treatment efficacy.

4.2 Mixture of kaolin–silicon application modulates leaf tissues thickness and the biochemical defence

The biochemical parameters, including photosynthetic pigments, soluble sugars, soluble proteins, and secondary metabolites, showed a clear beneficial response to Si and Kl treatments.

In 2023, although MiKS 2 and MiKS 3-treated plants had significantly higher chlorophyll content compared to MiKS 1-treated plants, the untreated control plants exhibited even greater chlorophyll levels (Table 4). This response in untreated plants might also indicate an overcompensation for the stress, which could result in lower overall efficiency in photosynthesis due to the lack of additional protective mechanisms like those provided by Si and Kl treatments (Anjum et al., 2011; Ashraf and Harris, 2013).

In 2024, no significant differences were observed among the different treatments. Thus, the enhanced photosynthetic performance observed is likely attributable to other factors than pigment concentration, as the treatments did not significantly increase photosynthetic pigments, such as chlorophylls. Nevertheless, the improvement in photosynthetic efficiency can be attributed to the broader physiological benefits conferred by Si and Kl applications, which contributed to optimizing the photosynthetic process under stress conditions (Ma and Yamaji, 2015; Coskun

et al., 2018; Dinis et al., 2018a). In fact, in the work carried out by Zuccarini (2008), Si application led to an increase in photosynthetic rate without significant changes in chlorophyll content, suggesting that Si may improve photosynthetic efficiency by maintaining cell membrane integrity and regulating stomatal conductance rather than by directly enhancing pigment levels. Regarding carotenoids, MiKS 2 exhibited higher levels during maturation in 2023, whereas at veraison, its levels were intermediate, falling below those of the control. However, by maturation in 2024, MiKS 4 had the highest carotenoid content. An increase in carotenoids benefits plants by protecting them from excess light, dissipating energy, and preventing damage to *PSII* (Pitawala et al., 2024). Additionally, their antioxidant properties help reduce oxidative stress caused by drought, heat, and intense radiation. Carotenoids also stabilize photosynthesis by improving light absorption and energy efficiency. In this way, plants with higher carotenoid levels are more resilient and productive under adverse conditions. In fact, a lower total carotenoid content is associated with a reduced availability of photoprotective pigments within the cells, limiting the plant's ability to effectively dissipate excess light energy and neutralize reactive oxygen species. As a result, plants with insufficient carotenoid levels are more susceptible to photodamage when exposed to environmental stresses, such as high light intensity, drought, or heat, ultimately compromising the integrity and efficiency of the photosynthetic apparatus (Pitawala et al., 2024).

Regarding to leaf biochemical attributes (Table 5), soluble sugars in MiKS 3-treated plants were significantly higher compared to untreated plants during both veraison and maturation stages, which indicates an enhanced ability to accumulate carbohydrates as a protective mechanism against summer stress. These sugars likely serve as energy reserves, helping the plant to manage stress. Similar results, with an increase of soluble sugar content, were observed in several studies after the Si application (Ding et al., 2007; Trejo-Téllez et al., 2020; Camargo et al., 2023) and Kl application (Bernardo et al., 2021), which can be attributed to improved photosynthetic efficiency, better water use efficiency, and enhanced protection against abiotic stresses, which may have led to higher carbohydrate production and accumulation in the plants. In the present study, the increase in soluble sugars was accompanied by higher levels of soluble proteins, particularly in MiKS 4-treated plants in 2024. Increases in soluble proteins could be essential for stress responses, aiding in cellular maintenance and enzymatic activities that mitigate damage caused by environmental stressors. In fact, this accumulation of soluble protein has been previously observed after Si (Ding et al., 2007; Trejo-Téllez et al., 2020; Dinis et al., 2024) and Kl applications (Brito et al., 2018; Dinis et al., 2018a; Dinis et al., 2020).

Regarding secondary metabolites (Table 5), significant increases in phenols, flavonoids, and *ortho*-diphenols were generally observed in treated plants across both phenological stages and years, except for total phenols at veraison 2024 (no significant differences) and *ortho*-diphenols at maturation in 2023 (where only MiKS 3 showed significantly higher levels compared to the control). These compounds are known for their antioxidant properties, playing a crucial role in protecting plants against oxidative damage induced by stress. The observed biochemical enhancements can be attributed to the synergistic effects of Si and Kl applications. Indeed, these compounds are widely recognized for boosting plant resistance to stress and promoting the synthesis of secondary metabolites (Jiang et al., 2022; Dinis et al., 2024; Paskovic et al., 2024).

The observed enhancement of antioxidant defences, photosynthetic capacity, and osmotic regulation in treated plants may be closely linked to hormonal modulation (Figure 5), particularly a slight reduction in abscisic acid (ABA) levels in MiKS 4 and an increase in MiKS 2-treated plants, and an increase in indole-3-acetic acid (IAA) in MiKS 3- and MiKS 4-treated plants. These hormonal adjustments likely contributed to greater growth plasticity and improved adaptability under stress conditions (Dinis et al., 2018b). Fast hormonal responses are essential for plant acclimation/adaptation at both the physiological and biochemical levels (Jesus et al., 2015). In the context of summer stress, which is typical in the Douro Region, stomatal closure represents a short-term adaptive response. This process is tightly regulated by a complex network of signalling pathways, including hormonal regulation (Moutinho-Pereira et al., 2004; Zhang et al., 2006; Wani et al., 2016). Specifically, ABA regulates stomatal opening and closure, as well as leaf growth. It is synthesized in the mature chloroplasts of leaves (Pei et al., 2000) and/or in drying roots, then transported via xylem to the leaves (Zhang et al., 2006; Correia et al., 2014). In the present work, plants treated with MiKS 4 exhibited the lowest ABA levels, reflecting the better water status and higher stomatal conductance of these plants (Figure 5). This observation is aligned with findings of other authors, who reported that Kl application can reduce ABA biosynthesis in grapevines (Dinis et al., 2018b; Frioni et al., 2020). Furthermore, a reduction in ABA levels was also observed following Si application (Helaly et al., 2017; Hosseini et al., 2017). Conversely, the increase in ABA levels observed in MiKS 2-treated plants may suggest a lower effectiveness in mitigating water stress, as ABA accumulation generally reflects drought perception and stomatal closure (Chaves et al., 2009).

IAA, the main auxin in plants, is a key hormone involved in regulating cell growth, development, and root patterning (Dinis et al., 2018b; Zhao, 2010). Thus, the increased IAA levels observed in MiKS 3and MiKS 4-treated plants (Figure 5) indicate enhanced growth and cell division, supporting overall plant development and stress resistance. This overproduction of IAA following Kl application suggests improved acclimation to environmental stresses, according to previous findings (Ke et al., 2015; Wani et al., 2016). Similarly, several studies have reported an increase in IAA content after Si application (Wani et al., 2016; Helaly et al., 2017; Mir et al., 2022).

JA is a key hormonal molecule that regulates both plant development and defence mechanisms. It also works as a stress hormone, playing a crucial role in how plants respond to environmental challenges such as salinity, drought, temperature fluctuations, and heavy metal toxicity (Raza et al., 2022). SA is a vital hormone that acts as a key signalling molecule, regulating both plant immunity and growth (Rivas-San and Plasencia, 2011; Li

et al., 2022). In this study, increases in both JA (all treatments) and SA levels (MiKS 2) (Figure 5) suggest an activation of defence pathways, with these hormones playing a key role in enhancing the plant's response to both biotic and abiotic stresses. In a study conducted on grapevine cv. Cabernet Sauvignon, Wang et al. (2022) also reported an increase in both hormones following Kl application. Similarly, Jang et al. (2018) observed that Si application led to an increase in both hormones, further corroborating the findings of the present study.

Regarding the histological parameters (Table 6), all treated plants generally exhibited thicker upper and lower cuticles, a feature that may enhance disease resistance and reduce water loss (Ferrón-Carrillo and Urrestarazu, 2021). Interestingly, Brito et al. (2019) found no significant differences in upper cuticle thickness following Kl application. The differences observed in this study are likely attributed to the Si deposition induced by Si application. Previous research has shown a similar trend, where Si application resulted in increased cuticle thickness (Pozo et al., 2015; Ferrón-Carrillo and Urrestarazu, 2021). Therefore, Si application appears to reduce membrane permeability and transpiration through the cuticle, ultimately improving the plant's water balance (Romero-Aranda et al., 2006), which is in accordance with the findings presented in the present study.

It is worth noting that the findings of this study were obtained using the red grape variety Touriga Franca. Therefore, it would be relevant to explore whether similar responses to the combined application of Si and Kl can be observed in other grape varieties, such as white ones. For instance, due to the differences in phenolic composition, cuticle thickness, and natural photoprotection, white cultivars may exhibit distinct physiological and biochemical responses under summer stress conditions. Future research could help clarify the broader applicability of this strategy across different grapevine types.

5 Conclusions

The combined application of Si and Kl, particularly through MiKS 2, MiKS 3, and MiKS 4 treatments, significantly enhanced grapevine ecophysiological and biochemical performance. The applied treatments improved water use efficiency, photosynthetic capacity, stress tolerance, and secondary metabolite production, while also inducing hormonal balance and anatomical adaptation, ultimately increasing plant resilience/adaptation to summer stress. The synergistic interaction between Si and Kl optimized physiological responses and can impact fruit quality, highlighting their potential as effective tools to enhance grapevine resilience in stressful environmental conditions. The present study also suggests that the integration of Si and Kl applications in vineyard management practices, particularly in drought-prone regions could be used as a beneficial cultural practice.

Considering all the parameters evaluated, MiKS 3 emerged as the most promising formulation, as it promoted significant improvements in plant performance while showing only minor differences when compared to MiKS 4. Therefore, the increased cost associated with the use of 8% Si in MiKS 4 may not be justified, given the similar outcomes achieved with the 6% Si concentration in MiKS 3.

Future research would consider the long-term impacts of these treatments on grape composition and wine quality across different grapevine types, including white varieties. Additionally, incorporating oxidative stress indicators such as total antioxidant capacity and malondialdehyde (MDA) levels would provide a more comprehensive understanding of the redox status and the protective mechanisms triggered by the combined application of Si and Kl under adverse climatic conditions.

Data availability statement

The original contributions presented in the study are included in the article/supplementary material. Further inquiries can be directed to the corresponding authors.

Author contributions

SdP: Data curation, Formal analysis, Investigation, Methodology, Resources, Software, Visualization, Writing – original draft. AM: Data curation, Formal analysis, Investigation, Methodology, Resources, Software, Visualization, Writing – review & editing. MB: Formal analysis, Investigation, Methodology, Software, Visualization, Writing – original draft. CM: Methodology, Writing – review & editing. SrP: Methodology, Writing – review & editing. MO: Methodology, Writing – review & editing. LP: Data curation, Formal Analysis, Investigation, Methodology, Visualization, Writing – original draft. IG: Methodology, Writing – review & editing. BS: Methodology, Writing – review & editing. ZB: Methodology, Writing – review & editing. RM: Methodology, Writing – review & editing. DB: Methodology, Writing – review & editing. JM: Conceptualization, Funding acquisition, Writing – review & editing. LD: Conceptualization, Funding acquisition, Project administration, Resources, Supervision, Validation, Writing – review & editing.

Funding

The author(s) declare that financial support was received for the research and/or publication of this article. This work was financed by Vine & Wine Portugal -Driving Sustainable Growth Through Smart Innovation, co-financed by the PRR -Plano de Recuperação e Resiliência e pelos Fundos Europeus NextGeneration EU, within the scope of "Agendas Mobilizadoras para a Reindustrialização", under ref. C644866286-00000011, under the subproject "New Products/formulations to promote a vine more resilience to climatic changes (Miks4Vine)". This work is supported by National Funds by FCT –Portuguese Foundation for Science and Technology, under the projects UID/04033/2023: Centre for the Research and Technology of Agro-Environmental and Biological Sciences and LA/P/0126/2020 (https://doi.org/10.54499/LA/P/0126/2020).

Acknowledgments

The authors gratefully acknowledge the support and collaboration of Engineer Tiago Maia from Quinta de Ventozelo, whose contribution was essential to the development of this work. The authors also acknowledge João Lourenço from TecniFerti for the provision of the products used in this study.

Conflict of interest

The authors declare that the research was conducted in the absence of any commercial or financial relationships that could be construed as a potential conflict of interest.

Generative AI statement

The author(s) declare that no Generative AI was used in the creation of this manuscript.

Publisher's note

All claims expressed in this article are solely those of the authors and do not necessarily represent those of their affiliated organizations, or those of the publisher, the editors and the reviewers. Any product that may be evaluated in this article, or claim that may be made by its manufacturer, is not guaranteed or endorsed by the publisher.

References

AbdAllah, A. (2017). Impacts of kaolin and pinoline foliar application on growth, yield and water use efficiency of tomato (*Solanum lycopersicum* L.) grown under water deficit: a comparative study. *J. Saudi Soc Agric. Sci.* 18, 256–268. doi: 10.1016/j.jssas.2017.08.001

Ahmed, M., Hassan, F., and Asif, M. (2014). Amelioration of drought in sorghum (*Sorghum bicolor* L.) by silicon. *Commun. Soil Sci. Plant Anal.* 45, 470–486. doi: 10.1080/00103624.2013.863907

Albetis, J., Jacquin, A., Goulard, M., Poilvé, H., Rousseau, J., Clenet, H., et al. (2018). On the potentiality of UAV multispectral imagery to detect flavescence dorée and grapevine trunk diseases. *Remote Sens.* 11, 23. doi: 10.3390/rs11010023

Ali, A., Tahir, M., Amin, M., Basra, S. M. A., Maqbool, M., and Lee, D. (2013). Si-induced stress tolerance in wheat (*Triticum aestivum* L.) hydroponically grown under water deficit conditions. *Bulg. J. Agric. Sci.* 19, 952–958. Available online at: https://www.researchgate.net/publication/272563912.

Amin, M., Ahmad, R., Basra, S., and Murtaza, G. (2014). Silicon induced improvement in morpho-physiological traits of maize (*Zea mays* L.) under water deficit. *Pak. J. Agric. Sci.* 51, 187–196.

Anjum, S. A., Xie, X. Y., Wang, L. C., Saleem, M. F., Man, C., and Lei, W. (2011). Morphological, physiological and biochemical responses of plants to drought stress. *Afr. J. Agric. Res.* 6, 2026–2032. doi: 10.5897/AJAR10.027

Arnon, D. I. (1949). Copper enzymes in isolated chloroplasts: polyphenol oxidase in *Beta vulgaris*. *Plant Physiol.* 24, 1–15. doi: 10.1104/pp.24.1.1

Ashraf, M., and Harris, P. J. C. (2013). Photosynthesis under stressful environments: an overview. *Photosynthetica.* 51, 163–190. doi: 10.1007/s11099-013-0021-6

Azuara, M., González, M. R., Mangas, R., and Martín, P. (2023). Kaolin foliar-application improves the photosynthetic performance and fruit quality of Verdejo grapevines. *Bio Web Conferences.* 68, 1024. doi: 10.1051/bioconf/20236801024

Bernardo, S., Dinis, L. T., Luzio, A., MaChado, N., Gonçalves, A., Vives-Peris, V., et al. (2021). Optimising grapevine summer stress responses and hormonal balance by applying kaolin in two Portuguese Demarcated Regions. *OENO One* 55 (1), 207–222. doi: 10.20870/oeno-one.2021.55.1.4502

Bernardo, S., Dinis, L. T., MaChado, N., Barros, A., Pitarch-Bielsa, M., Malheiro, A. C., et al. (2022). Uncovering the effects of kaolin on balancing berry phytohormones and quality attributes of *Vitis vinifera* grown in warm-temperate climate regions. *J. Sci. Food Agric.* 102, 782–793. doi: 10.1002/jsfa.11413

Bilger, W., and Schreiber, U. (1986). Energy-dependent quenching of dark-level chlorophyll fluorescence in intact leaves. *Photosynth. Res.* 10, 303–308. doi: 10.1007/BF00118295

Boari, F., Donadio, A., Schiattone, M. I., and Cantore, V. (2015). Particle film technology: a supplemental tool to save water. *Agric. Water Manage.* 147, 154–162. doi: 10.1016/j.agwat.2014.07.014

Bradford, M. M. (1976). A rapid and sensitive method for the quantitation of microgram quantities of protein utilizing the principle of protein-dye binding. *Anal. Biochem.* 72, 248–254. doi: 10.1016/0003-2697(76)90527-3

Brito, C., Dinis, L. T., Ferreira, H., Rocha, L., Pavia, L., Moutinho-Pereira, J., et al. (2018). Kaolin particle film modulates morphological, physiological and biochemical olive tree responses to cyclic water deficit. *Plant Physiol. Biochem.* 133, 29–39. doi: 10.1016/j.plaphy.2018.10.028

Brito, C., Dinis, L. T., Luzio, A., Silva, E., Gonçalves, A., Meijón, M., et al. (2019). Kaolin and salicylic acid alleviate summer stress in rainfed olive orchards by modulation of distinct physiological and biochemical responses. *Sci. Hortic.* 246, 201–211. doi: 10.1016/j.scienta.2018.10.059

Cabello-Pasini, A., and Macías-Carranza, V. (2011). Optical properties of grapevine leaves: reflectance, transmittance, absorptance and chlorophyll concentration. *Agrocienc.* 45, 943–957. Available online at: https://www.researchgate.net/publication/287889758.

Camargo, M. S., Baltieri, G. J., Santos, H. L., Carnietto, M. R. A., Reis, A. R., Pacheco, A. C., et al. (2023). Silicon fertilization enhances photosynthetic activity and sugar metabolism in sugarcane cultivars under water deficit at the ripening phase. *Silicon.* 15, 3021–3033. doi: 10.1007/s12633-022-02236-y

Carvalho, L. C., Coito, J. L., Colaço, S., Sangiogo, M., and Amâncio, S. (2015). Heat stress in grapevine: the pros and cons of acclimation. *Plant Cell Environ.* 38, 777–789. doi: 10.1111/pce.12445

Cataldo, E., Fucile, M., and Mattii, G. B. (2022). Effects of kaolin and shading net on the ecophysiology and berry composition of Sauvignon Blanc grapevines. *Agriculture.* 12, 491. doi: 10.3390/agriculture12040491

Chaves, M. M., Flexas, J., and Pinheiro, C. (2009). Photosynthesis under drought and salt stress: regulation mechanisms from whole plant to cell. *Ann. Bot.* 103, 551–560. doi: 10.1093/aob/mcn125

Conde, A., Neves, A., Breia, R., Pimentel, D., Dinis, L. T., Bernardo, S., et al. (2018). Kaolin particle film application stimulates photoassimilate synthesis and modifies the primary metabolome of grape leaves. *J. Plant Physiol.* 223, 47–56. doi: 10.1016/j.jplph.2018.02.004

Conde, A., Pimentel, D., Neves, A., Dinis, L. T., Bernardo, S., Correia, C. M., et al. (2016). Kaolin foliar application has a stimulatory effect on phenylpropanoid and flavonoid pathways in grape berries. *Front. Plant Sci.* 7. doi: 10.3389/fpls.2016.01150

Correia, B., Pintó-Marijuan, M., Neves, L., Brossa, R., Dias, M. C., Costa, A., et al. (2014). Water stress and recovery in the performance of two *Eucalyptus globulus* clones: physiological and biochemical profiles. *Physiol. Plant* 150, 580–592. doi: 10.1111/ppl.12110

Coskun, D., Deshmukh, R., Sonah, H., Menzies, J. G., Reynolds, O., Ma, J. F., et al. (2018). The controversies of silicon's role in plant biology. *New Phytol.* 221, 67–85. doi: 10.1111/nph.15343

Dayer, S., Prieto, J. A., Galat, E., and Perez, P. J. (2013). Carbohydrate reserve status of Malbec grapevines after several years of regulated deficit irrigation and crop load regulation. *Aust. J. Grape Wine Res.* 19, 422–430. doi: 10.1111/ajgw.12044

Dayer, S., Prieto, J. A., Galat, E., and Perez, P. J. (2016). Leaf carbohydrate metabolism in Malbec grapevines: combined effects of regulated deficit irrigation and crop load. *Aust. J. Grape Wine Res.* 22, 115–123. doi: 10.1111/ajgw.12180

Dehghanipoodeh, S., Ghobadi, C., Baninasab, B., Gheysari, M., and Shiranibidabadi, S. (2018). Effect of silicon on growth and development of strawberry under water deficit conditions. *Hortic. Plant J.* 4, 226–232. doi: 10.1016/j.hpj.2018.09.004

Denaxa, N.-K., Roussos, P. A., Damvakaris, T., and Stournaras, V. (2012). Comparative effects of exogenous glycine betaine, kaolin clay particles and Ambiol on photosynthesis, leaf sclerophylly indexes and heat load of olive cv. Chondrolia Chalkidikis under drought. *Sci. Hortic.* 137, 87–94. doi: 10.1016/j.scienta.2012.01.012

Ding, Y., Liang, Y., Zhu, J., and Li, Z. (2007). Effects of silicon on plant growth, photosynthetic parameters and soluble sugar content in leaves of wheat under drought stress. *J. Plant Nutr. Fertil.* 13, 471–478. doi: 10.11674/zwyf.2007.0319

Dinis, L. T., Bernardo, S., Luzio, A., Pinto, G., Meijón, M., Pintó-Marijuan, M., et al. (2018a). Kaolin modulates ABA and IAA dynamics and physiology of grapevine under

Mediterranean summer stress. *J. Plant Physiol.* 220, 181–192. doi: 10.1016/j.jplph.2017.11.007

Dinis, L. -T., Bernardo, S., Matos, C., Malheiro, A., Flores, R., Alves, S., et al. (2020). Overview of Kaolin outcomes from vine to wine: cerceal white variety case study. *Agronomy.* 10 (9), 1422. doi: 10.3390/agronomy10091422

Dinis, L. T., Ferreira, H., Pinto, G., Bernardo, S., Correia, C. M., and Moutinho-Pereira, J. (2016). Kaolin-based, foliar reflective film protects photosystem II structure and function in grapevine leaves exposed to heat and high solar radiation. *Photosynthetica.* 54, 47–55. doi: 10.1007/s11099-015-0156-8

Dinis, L. T., Malheiro, A. C., Luzio, A., Fraga, H., Ferreira, H., Gonçalves, I., et al. (2018b). Improvement of grapevine physiology and yield under summer stress by kaolin-foliar application: Water relations, photosynthesis and oxidative damage. *Photosynthetica.* 56, 641–651. doi: 10.1007/s11099-017-0714-3

Dinis, L. T., Mota, N., Martins, S., Ribeiro, A., Moutinho-Pereira, J., and Pereira, S. (2024). Foliar silicon application in the era of climate change as a part of strategy to mitigate summer stress in Mediterranean viticulture: A comparative study in Touriga Franca grapevine. *Horticulturae.* 10, 1224. doi: 10.3390/horticulturae10111224

Durgbanshi, A., Arbona, V., Pozo, O., Miersch, O., Sancho, J. V., and Gomez-Cadenas, A. (2005). Simultaneous determination of multiple phytohormones in plant extracts by liquid chromatography-electrospray tandem mass spectrometry. *J. Agric. Food Chem.* 53, 8437–8442. doi: 10.1021/jf050884b

Edwards, E. J., Smithson, L., Graham, D. C., and Clingeleffer, P. R. (2011). Grapevine canopy response to a high-temperature event during deficit irrigation. *Aust. J. Grape Wine Res.* 17, 153–161. doi: 10.1111/j.1755-0238.2011.00125.x

Epstein, E. (1994). The anomaly of silicon in plant biology. *Proc. Natl. Acad. Sci. United States America.* 91, 11–17. doi: 10.1073/pnas.91.1.11

Etesami, H., and Jeong, B. R. (2018). Silicon (Si): Review and future prospects on the action mechanisms in alleviating biotic and abiotic stresses in plants. *Ecotoxicol. Environ. Saf.* 147, 881–896. doi: 10.1016/j.ecoenv.2017.09.063

Ferrón-Carrillo, F., and Urrestarazu, M. (2021). Effects of Si in nutrient solution on leaf cuticles. *Sci. Hortic.* 278, 109863. doi: 10.1016/j.scienta.2020.109863

Flexas, J., Bota, J., Escalona, J. M., Sampol, B., and Medrano, H. (2002). Effects of drought on photosynthesis in grapevines under field conditions: an evaluation of stomatal and mesophyll limitations. *Funct. Plant Biol.* 29, 461–471. doi: 10.1071/PP01119

Frioni, T., Tombesi, S., Sabbatini, P., Squeri, C., Lavado, R. N., Palliotti, A., et al. (2020). Kaolin reduces ABA biosynthesis through the inhibition of neoxanthin synthesis in grapevines under water deficit. *Int. J. Mol. Sci.* 21, 4950. doi: 10.3390/ijms21144950

Galat, G. E., Sadras, V. O., Keller, M., and Perez, P. J. (2019). Interactive effects of high temperature and water deficit on Malbec grapevines. *Aust. J. Grape Wine Res.* 25, 345–356. doi: 10.1111/ajgw.12398

Genty, B., Briantais, J. M., and Baker, N. R. (1989). The relationship between the quantum yield of photosynthetic electron transport and quenching of chlorophyll fluorescence. *Biochim. Biophys. Acta – Gen. Subjects.* 990, 87–92. doi: 10.1016/S0304-4165(89)80016-9

Giorgi, E. G., Sadras, V. O., Keller, M., and Peña, J. P.. (2019). Interactive effects of high temperature and water deficit on Malbec grapevines. *Aust. J. Grape Wine Res.* 25, 345–356. doi: 10.1111/ajgw.12398

Glenn, D. M., Cooley, N. M., Walker, R. R., Clingeleffer, P., and Shellie, K. (2010). Impact of kaolin particle film and water deficit on wine grape water use efficiency and plant water relations. *HortScience* 45, 1178–1187. doi: 10.21273/HORTSCI.45.8.1178

Gong, H. J., and Chen, K. M. (2012). The regulatory role of silicon on water relations, photosynthetic gas exchange, and carboxylation activities of wheat leaves in field drought conditions. *Acta Physiol. Plant* 34, 1589–1594. doi: 10.1007/s11738-012-0954-6

Gong, H. J., Chen, K. M., Chen, G. C., Wang, S. M., and Zhang, C. L. (2003). Effects of silicon on growth of wheat under drought. *J. Plant Nutr.* 26, 1055–1063. doi: 10.1081/PLN-120020075

Granato, D., Margraf, T., Brotzakis, I., Capuano, E., and Van Ruth, S. M. (2015). Characterization of conventional, biodynamic, and organic purple grape juices by chemical markers, antioxidant capacity, and instrumental taste profile. *J. Food Sci.* 80, 55–65. doi: 10.1111/1750-3841.12722

Gunes, A., Kadioglu, Y. K., Pilbeam, D. J., Inal, A., Coban, S., and Aksu, A. (2008). Influence of silicon on sunflower cultivars under drought stress, II: Essential and nonessential element uptake determined by polarized energy dispersive X-ray fluorescence. *Commun. Soil Sci. Plant Anal.* 39, 1904–1927. doi: 10.1080/00103620802134719

Gutiérrez-Gamboa, G., Zheng, W., and Martínez de Toda, F. (2021). Current viticultural techniques to mitigate the effects of global warming on grape and wine quality: A comprehensive review. *Food Res. Int.* 139, 109946. doi: 10.1016/j.foodres.2020.109946

Hattori, T., Sonobe, K., Inanaga, S., An, P., Tsuji, W., Araki, H., et al. (2007). Short-term stomatal responses to light intensity changes and osmotic stress in sorghum seedlings raised with and without silicon. *Environ. Exp. Bot.* 60, 177–182. doi: 10.1016/j.envexpbot.2006.10.004

Helaly, M. N., El-Hoseiny, H., El-Sheery, N. I., Rastogi, A., and Kalaji, H. M. (2017). Regulation and physiological role of silicon in alleviating drought stress of mango. *Plant Physiol. Biochem.* 118, 31–44. doi: 10.1016/j.plaphy.2017.05.021

Hosseini, S. A., Maillard, A., Hajirezaei, M. R., Ali, N., Schwarzenberg, A., Jamois, F., et al. (2017). Induction of barley silicon transporter HvLsi1 and HvLsi2, increased silicon concentration in the shoot and regulated stress response. *Front. Plant Sci.* 8. doi: 10.3389/fpls.2017.01359

Iacono, F., Buccella, A., and Peterlunger, E. (1998). Water stress and rootstock influence on leaf gas exchange of grafted and ungrafted grapevines. *Sci. Hortic.* 75, 27–39. doi: 10.1016/S0304-4238(98)00113-7

Idso, S., Jackson, R., Pinter, P. Jr., Reginato, R., and Hatfield, J. (1981). Normalizing the stress-degree-day parameter for environmental variability. *Agric. Meteorol.* 24, 45–55. doi: 10.1016/0002-1571(81)90032-7

Instituto Português do Mar e da Atmosfera (IPMA) (2024). Boletim climatológico anual 2023 (Instituto Português do Mar e da Atmosfera). Available online at: https://www.ipma.pt/pt/media/noticias/news.detail.jsp?f=boletim-climatologico-anual-2023.html&y=2024.

Jain, R., Singh, S. P., Singh, A., Singh, S., Tripathi, P., Kishor, R., et al. (2017). Changes in growth, yield, juice quality and biochemical attributes of sugarcane in response to orthosilicic acid granules. *Sugar Tech.* 19, 300–304. doi: 10.1007/s12355-016-0469-3

Jang, S. W., Kim, Y., Khan, A. L., Na, C. I., and Lee, I. J. (2018). Exogenous short-term silicon application regulates macro-nutrients, endogenous phytohormones, and protein expression in *Oryza sativa* L. *BMC Plant Biol.* 18, 4. doi: 10.1186/s12870-017-1216-y

Jesus, C., Meijón, M., Monteiro, P., Correia, B., Amaral, J., Escandón, M., et al. (2015). Salicylic acid application modulates physiological and hormonal changes in *Eucalyptus globulus* under water deficit. *Environ. Exp. Bot.* 118, 56–66. doi: 10.1016/j.envexpbot.2015.06.004

Jiang, H., Song, Z., Su, Q. W., Wei, Z. H., Li, W. C., Jiang, Z. X., et al. (2022). Transcriptomic and metabolomic reveals silicon enhances adaptation of rice under dry cultivation by improving flavonoid biosynthesis, osmoregulation, and photosynthesis. *Front. Plant Sci.* 13. doi: 10.3389/fpls.2022.967537

Jifon, J. L., and Syvertsen, J. P. (2003). Kaolin particle film applications can increase photosynthesis and water use efficiency of 'Ruby Red' grapefruit leaves. *J. Amer. Soc Hortic. Sci.* 128, 107–112. doi: 10.21273/JASHS.128.1.0107

Ju, Y., Yang, B. H., He, S., Tu, T. Y., Min, Z., Fang, Y. L., et al. (2019). Anthocyanin accumulation and biosynthesis are modulated by regulated deficit irrigation in Cabernet Sauvignon (*Vitis vinifera* L.) grapes and wines. *Plant Physiol. Biochem.* 135, 469–479. doi: 10.1016/j.plaphy.2018.11.013

Ke, Q., Wang, Z., Ji, C. Y., Jeong, J. C., Lee, H. S., Li, H., et al. (2015). Transgenic poplar expressing Arabidopsis YUCCA6 exhibits auxin-overproduction phenotypes and increased tolerance to abiotic stress. *Plant Physiol. Biochem.* 94, 19–27. doi: 10.1016/j.plaphy.2015.05.003

Keller, M. (2020). *The Science of Grapevines. 3rd ed* (London: Elsevier Academic Press).

Keller, M., Romero, P., Gohil, H., Smithyman, R. P., Riley, W. R., Casassa, F., et al. (2016). Deficit irrigation alters grapevine growth, physiology, and fruit microclimate. *AJEV.* 67, 426–435. doi: 10.5344/ajev.2016.16032

Khan, W. U. D., Aziz, T., Hussain, I., Ramzani, P. M. A., and Reichenauer, T. G. (2017). Silicon: a beneficial nutrient for maize crop to enhance photochemical efficiency of photosystem II under salt stress. *Arch. Agron. Soil Sci.* 63, 599–611. doi: 10.1080/03650340.2016.1233322

Kok, D., and Bal, E. (2018). Leaf removal treatments combined with kaolin particle film technique from different directions of grapevine's canopy affect the composition of phytochemicals of cv. Muscat Hamburg (*Vitis vinifera* L.). *Erwerbs-Obstbau* 60(8), 1–7. doi: 10.1007/s10341-017-0337-7

Kurdali, F., Mohammad, A. C., and Ahmad, M. (2013). Growth and nitrogen fixation in silicon and/or potassium-fed chickpeas grown under drought and well-watered conditions. *J. Stress Physiol. Biochem.* 9, 385–406.

Laane, H.-M. (2018). The effects of foliar sprays with different silicon compounds. *Plants.* 7, 45. doi: 10.3390/plants7020045

Levin, A. D. (2019). Re-evaluating pressure chamber methods of water status determination in field-grown grapevine (*Vitis* spp.). *Agric. Water Manage.* 221, 422–429. doi: 10.1016/j.agwat.2019.03.026

Leyva, A., Quintana, A., Sánchez, M., Rodríguez, E. N., Cremata, J., and Sánchez, J. C. (2008). Rapid and sensitive anthrone–sulfuric acid assay in microplate format to quantify carbohydrate in biopharmaceutical products: method development and validation. *Biologicals.* 36, 134–141. doi: 10.1016/j.biologicals.2007.09.001

Li, A., Sun, X., and Liu, L. (2022). Action of salicylic acid on plant growth. *Front. Plant Sci.* 13. doi: 10.3389/fpls.2022.878076

Li, J., Guan, Y., Yuan, L., Hou, J., Wang, C., Liu, F., et al. (2019). Effects of exogenous IAA in regulating photosynthetic capacity, carbohydrate metabolism and yield of Zizania latifolia. *Sci. Hortic.* 253, 276–285. doi: 10.1016/j.scienta.2019.04.058

Lichtenthaler, H. K. (1987). Chlorophylls and carotenoids: pigments of photosynthetic biomembranes. *Methods Enzymol.* 148, 350–382. doi: 10.1016/0076-6879(87)48036-1

Luzio, A., Bernardo, S., Correia, C., Moutinho-Pereira, J., and Dinis, L. T. (2021). Phytochemical screening and antioxidant activity on berry, skin, pulp and seed from seven red Mediterranean grapevine varieties (*Vitis vinifera* L.) treated with kaolin foliar sunscreen. *Sci. Hortic.* 281, 109962. doi: 10.1016/j.scienta.2021.109962

Ma, C. C., Li, Q. F., Gao, Y. B., and Xin, T. R. (2004). Effects of silicon application on drought resistance of cucumber plants. *Soil Sci. Plant Nutri.* 50, 623–632. doi: 10.1080/00380768.2004.10408520

Ma, J. F., and Yamaji, N. (2015). A cooperative system of silicon transport in plants. *Trends Plant Sci.* 20, 435–442. doi: 10.1016/j.tplants.2015.04.007

Magalhães, N. (2015). *Tratado de Viticultura – A Videira, A Vinha e o Terroir. 2nd ed* (Lisboa, Portugal: Chaves-Ferreira), ISBN: .

Maghsoudi, K., Emam, Y., and Ashraf, M. (2015). Influence of foliar application of silicon on chlorophyll fluorescence, photosynthetic pigments, and growth in water-stressed wheat cultivars differing in drought tolerance. *Turk J. Bot.* 39, 625–634. doi: 10.3906/bot-1407-11

Marinari, S., Calfapietra, C., De Angelis, P., Mugnozza, G. S., and Grego, S. (2007). Impact of elevated CO_2 and nitrogen fertilization on foliar elemental composition in a short rotation poplar plantation. *Environ. pollut.* 147, 507–515. doi: 10.1016/j.envpol.2006.08.041

Medrano, H., Escalona, J. M., Cifre, J., Bota, J., and Flexas, J. (2003). A ten-year study on the physiology of two Spanish grapevine cultivars under field conditions: effects of water availability from leaf photosynthesis to grape yield and quality. *Funct. Plant Biol.* 30, 607–619. doi: 10.1071/FP02110

Ming, D. F., Pei, Z. F., Naeem, M. S., Gong, H. J., and Zhou, W. J. (2012). Silicon alleviates PEG-induced water-deficit stress in upland rice seedlings by enhancing osmotic adjustment. *J. Agron. Crop Sci.* 198, 14–26. doi: 10.1111/j.1439-037X.2011.00486.x

Mir, R. A., Bhat, B. A., Yousuf, H., Islam, S. T., Rizvi, M. A., Charagh, S., et al. (2022). Multidimensional role of silicon to activate resilient plant growth and to mitigate abiotic stress. *Front. Plant Sci.* 13. doi: 10.3389/fpls.2022.819658

Moutinho-Pereira, J. M., Correia, C. M., Gonçalves, B. M., Bacelar, E. A., and Torres-Pereira, J. M. (2004). Leaf gas exchange and water relations of grapevines grown in three different conditions. *Photosynthetica.* 42, 81–86. doi: 10.1023/B:PHOT.0000040573.09614.1d

Muller, J. L., Rattunde, R., Ribler, S., Liedel, K., Benade, F., Rost, A., et al. (2021). Two Auxinic Herbicides Affect Brassica napus Plant Hormone Levels and Induce Molecular Changes in Transcription. *Biomolecules* 11 (8), 1153. doi: 10.3390/biom11081153

Murakami, A., Kim, E., Minagawa, J., and Takizawa, K. (2024). How much heat does non-photochemical quenching produce? *Front. Plant Sci.* 15. doi: 10.3389/fpls.2024.1367795

Nanos, P. G. (2015). Leaf and fruit responses to kaolin particle film applied onto mature olive trees. *JBAH.* 5, 17–27.

Nascimento, C. W. A., da Silva, F. B. V., Lima, L. H. V., Silva, J. R., de Lima Veloso, V., da Silva, F. L., et al. (2022). Silicon application to soil increases the yield and quality of table grapes (*Vitis vinifera* L.) grown in a semiarid climate of Brazil. *Silicon.* 15, 1647–1658. doi: 10.21203/rs.3.rs-1828772/v1

Ojeda, H., Deloire, A., and Carbonneau, A. (2001). Influence of water deficits on grape berry growth. *Vitis – J. Grapevine Res.* 40, 141–145. doi: 10.5073/vitis.2001.40.141-145

Okhrimenko, M., Coburn, C., and Hopkinson, C. (2019). Multi-Spectral Lidar: Radiometric calibration, canopy spectral reflectance, and vegetation vertical SVI profiles. *Remote Sens.* 11, 1556. doi: 10.3390/rs11131556

Oliva, K. M. E., Nascimento, C. W. A., Silva, F. B. V., Araújo, P. R. M., Oliveira, E. C. A., Feitosa, M. M., et al. (2020). Biomass and concentration of nutrients and silicon in sugarcane grown on soil fertilized with diatomite. *Rev. Bras. Ciências Agrárias.* 15, 1–7. doi: 10.5039/agraria.v15i4a8755

Pádua, L., Bernardo, S., Dinis, L. T., Correia, C., Moutinho-Pereira, J., and Sousa, J. J. (2022). The efficiency of foliar kaolin spray assessed through UAV-based thermal infrared imagery. *Remote Sens.* 14, 4019. doi: 10.3390/rs14164019

Paskovic, M. P., Custic, M. H., Lukic, I., Marcelic, S., Zurga, P., Vidovic, N., et al. (2024). Foliar nutrition strategies for enhancing phenolic and amino acid content in olive leaves. *Plants* 13 (24), 3514. doi: 10.3390/plants13243514

Pei, Z. M., Murata, Y., Benning, G., Thomine, S., Klusener, B., Allen, G. J., et al. (2000). Calcium channels activated by hydrogen peroxide mediate abscisic acid signalling in guard cells. *Nature.* 406, 731–734. doi: 10.1038/35021067

Pereira, S., Monteiro, A., Moutinho-Pereira, J., and Dinis, L. (2024). Silicon, an emergent strategy to lighten the effects of (a)biotic stresses on crops: a review. *J. Agron. Crop Sci.* 210, e12762. doi: 10.1111/jac.12762

Pilon, C., Soratto, R. P., and Moreno, L. A. (2013). Effects of soil and foliar application of soluble silicon on mineral nutrition, gas exchange, and growth of potato plants. *Crop Sci.* 53, 1605–1614. doi: 10.2135/cropsci2012.10.0580

Pitawala, S., Trifunovic, Z., Crosbie, N. D., Scales, P. J., and Martin, G. J. O. (2024). Biochemical changes due to photothermal acclimation of *Oedogonium* and associated implications for photosynthetic growth and biomass utilisation. *Algal Res.* 82, 103666. doi: 10.1016/j.algal.2024.103666

Pozo, K., Urrestarazu, M., Morales, I., Sánchez, J., Santos, M., Dianez, F., et al. (2015). Effects of silicon in the nutrient solution for three horticultural plant families on the vegetative growth, cuticle, and protection against *Botrytis cinérea*. *HortSci.* 50, 1447–1452. doi: 10.21273/HORTSCI.50.10.1447

Prichard, T., Hanson, B., Schwankl, L., Verdegaal, P., and Smith, R. (2004). *Deficit irrigation of quality winegrapes using micro-irrigation techniques* (Lodi, CA, USA: University of California Davis).

Qin, L., Kang, W. H., Qi, Y. L., Zhang, Z. W., and Wang, N. (2016). The influence of silicon application on growth and photosynthesis response of salt-stressed grapevines (*Vitis vinifera* L.). *Acta Physiol. Plant* 38, 68. doi: 10.1007/s11738-016-2087-9

Rastogi, A., Yadav, S., Hussain, S., Kataria, S., Hajihashemi, S., Kumari, P., et al. (2021). Does silicon really matter for the photosynthetic machinery in plants? *Plant Physiol. Biochem.* 169, 40–48. doi: 10.1016/j.plaphy.2021.11.004

Raza, A., Salehi, H., Rahman, M. A., Zahid, Z., Madadkar, H. M., Najafi-Kakavand, S., et al. (2022). Plant hormones and neurotransmitter interactions mediate antioxidant defenses under induced oxidative stress in plants. *Front. Plant Sci.* 13. doi: 10.3389/fpls.2022.961872

Rivas-San, V. M., and Plasencia, J. (2011). Salicylic acid beyond defence: its role in plant growth and development. *J. Exp. Bot.* 62, 3321–3338. doi: 10.1093/jxb/err031

Rizwan, M., Ali, S., Ibrahim, M., Farid, M., Adrees, M., Bharwana, S. A., et al. (2015). Mechanisms of silicon-mediated alleviation of drought and salt stress in plants: a review. *Environ. Sci. pollut. Res.* 22, 15416–15431. doi: 10.1007/s11356-015-5305-x

Rocheta, M., Becker, J., Coito, J., Carvalho, L., and Amâncio, S. (2014). Heat and water stress induce unique transcriptional signatures of heat-shock proteins and transcription factors in grapevine. *Funct. Integr. Genomics* 14, 135–148. doi: 10.1007/s10142-013-0338-z

Rodrigues, L., Santana, I., Coelho, R., Murta, G., Cardoso, H., Campos, C., et al. (2025). Exploring *Opuntia ficus-indica* as a strategy to mitigate high temperatures effects in vineyards: Insights into physiological and proteomic responses. *Agronomy* 15, 869. doi: 10.3390/agronomy15040869

Rodrigues, M. J., Soszynski, A., Martins, A., Rauter, A. P., Neng, N. R., Nogueira, J. M., et al. (2015). Unravelling the antioxidant potential and the phenolic composition of different anatomical organs of the marine halophyte *Limonium algarvense*. *Ind. Crops Prod.* 77, 315–322. doi: 10.1016/j.indcrop.2015.08.061

Romero-Aranda, M. R., Jurado, O., and Cuartero, J. (2006). Silicon alleviates the deleterious salt effect on tomato plant growth by improving plant water status. *J. Plant Physiol.* 163, 847–855. doi: 10.1016/j.jplph.2005.05.010

Rosati, A., Melcalf, S. G., Buchner, R. P., Fulton, A. E., and Lampinen, B. D. (2006). Effects of kaolin application on light absorption and distribution, radiation use efficiency and photosynthesis of almond and walnut canopies. *Ann. Bot.* 99, 255–263. doi: 10.1093/aob/mcl252

Sadras, V. O., Montoro, A., Moran, M. A., and Aphalo, P. J. (2012). Elevated temperature altered the reaction norms of stomatal conductance in field-grown grapevine. *Agric. For. Meteorol.* 165, 35–42. doi: 10.1016/j.agrformet.2012.06.005

Sadras, V. O., and Soar, C. J. (2009). Shiraz vines maintain yield in response to a 2–4 °C increase in maximum temperature using an open-top heating system at key phenostages. *Eur. J. Agron.* 31, 250–258. doi: 10.1016/j.eja.2009.09.004

Schabl, P., Gabler, C., Kührer, E., and Wenzel, W. (2020). Effects of silicon amendments on grapevine, soil and wine. *Plant Soil Environ.* 66, 403–414. doi: 10.17221/40/2020-PSE

Scholander, P. F., Hammel, H. T., Bradstreet, E. D., and Hemmingsen, E. A. (1965). Sap pressure in vascular plants: negative hydrostatic pressure can be measured in plants. *Sci.* 148, 339–346. doi: 10.1126/science.148.3668.339

Segura-Monroy, S., Uribe-Vallejo, A., Ramirez-Godoy, A., and Restrepo-Diaz, H. (2015). Effect of kaolin application on growth, water use efficiency, and leaf epidermis characteristics of *Physalis Peruviana* L. seedlings under two irrigation regimes. *J. Agric. Sci. Technol.* 17, 1585–1596. Available online at: https://www.researchgate.net/publication/282976386.

Sharma, R., Reddy, S. V. R., and Datta, S. C. (2015). Particle films and their applications in horticultural crops. *Appl. Clay Sci.* 116–117, 54–68. doi: 10.1016/j.clay.2015.08.009

Shellie, K. C., and King, B. A. (2012). Kaolin-based foliar reflectant and water deficit influence Malbec leaf and berry temperature, pigments, and photosynthesis. *AJEV.* 63, 12115. doi: 10.5344/ajev.2012.12115

Soar, C. J., Collins, M. J., and Sadras, V. O. (2009). Irrigated Shiraz vines (*Vitis vinifera*) upregulate gas exchange and maintain berry growth in response to short spells of high maximum temperature in the field. *Funct. Plant Biol.* 36, 801–814. doi: 10.1071/FP09101

Suter, B., Destrac, I. A., Gowdy, M., Dai, Z., and van Leeuwen, C. (2021). Adapting wine grape ripening to global change requires a multi-trait approach. *Front. Plant Sci.* 12. doi: 10.3389/fpls.2021.624867

Trejo-Téllez, L. I., García-Jiménez, A., Escobar-Sepúlveda, H. F., Ramírez-Olvera, S. M., Bello-Bello, J. J., and Gómez-Merino, F. C. (2020). Silicon induces hormetic dose-response effects on growth and concentrations of chlorophylls, amino acids and sugars in pepper plants during the early developmental stage. *PeerJ.* 8, e9224. doi: 10.7717/peerj.9224

Tripathi, D. K., Singh, S., Singh, V. P., Prasad, S. M., Dubey, N. K., and Chauhan, D. K. (2017). Silicon nanoparticles more effectively alleviated UV-B stress than silicon in wheat (*Triticum aestivum*) seedlings. *Plant Physiol. Biochem.* 110, 70–81. doi: 10.1016/j.plaphy.2016.06.026

Tuccio, L., Piccolo, E. L., Battelli, R., Matteoli, S., Massai, R., Scalabrelli, G., et al. (2019). Physiological indicators to assess water status in potted grapevine (*Vitis vinifera* L.). *Sci. Hortic.* 255, 8–13. doi: 10.1016/j.scienta.2019.05.017

Venios, X., Korkas, E., Nisiotou, A., and Banilas, G. (2020). Grapevine responses to heat stress and global warming. *Plants.* 9, 1754. doi: 10.3390/plants9121754

Von Caemmerer, S., and Farquhar, G. D. (1981). Some relationships between the biochemistry of photosynthesis and the gas exchange of leaves. *Planta.* 153, 376–387. doi: 10.1007/BF00384257

Wang, Y., Cao, X., Han, Y., Han, X., Wang, Z., Xue, T., et al. (2022). Kaolin particle film protects Grapevine cv. Cabernet Sauvignon against downy mildew by forming a

particle film at the leaf surface, directly acting on sporangia and inducing the defense of the plant. *Front. Plant Sci.* 12. doi: 10.3389/fpls.2021.796545

Wang, D., Hou, L., Zhang, L., and Liu, P. (2021). The mechanisms of silicon on maintaining water balance under water deficit stress. *Physiol. Plant* 173, 1253–1262. doi: 10.1111/ppl.13520

Wani, S. H., Kumar, V., Shriram, V., and Sah, S. K. (2016). Phytohormones and their metabolic engineering for abiotic stress tolerance in crop plants. *Crop J.* 4, 162–176. doi: 10.1016/j.cj.2016.01.010

Yang, B., He, S., Liu, Y., Liu, B., Ju, Y., Kang, D., et al. (2020). Transcriptomics integrated with metabolomics reveals the effect of regulated deficit irrigation on anthocyanin biosynthesis in Cabernet Sauvignon grape berries. *Food Chem.* 314, 126170. doi: 10.1016/j.foodchem.2020.126170

Zhang, J., Jia, W., Yang, J., and Ismail, A. M. (2006). Role of ABA in integrating plant responses to drought and salt stresses. *Field Crops Res.* 97, 111–119. doi: 10.1016/j.fcr.2005.08.018

Zhao, Y. (2010). Auxin biosynthesis and its role in plant development. *Annu. Rev. Plant Biol.* 61, 49–64. doi: 10.1146/annurev-arplant-042809-112308

Zhu, R., Hu, T., Zhang, Q., Zeng, X., Zhou, S., Wu, F., et al. (2023). A stomatal optimization model adopting a conservative strategy in response to soil moisture stress. *J. Hydrol* 617, 128931. doi: 10.1016/j.jhydrol.2022.128931

Zuccarini, P. (2008). Effects of silicon on photosynthesis, water relations and nutrient uptake of *Phaseolus vulgaris* under NaCl stress. *Biol. Plant* 52, 157–160. doi: 10.1007/s10535-008-0034-3